Title

Obscurin and KCTD6 regulate cullin-dependent small ankyrin-1 (sAnk1.5) protein turnover

Journal

Molecular Biology of the Cell, 23(13)

ISSN

1059-1524

Authors

Lange, Stephan
Perera, Sue
Teh, Phildrich
et al.

Publication Date

2012-07-01

DOI

10.1091/mbc.e12-01-0052

Peer reviewed

Obscurin and KCTD6 regulate cullin-dependent small ankyrin-1 (sAnk1.5) protein turnover

Stephan Lange[a], Sue Perera[b], Phildrich Teh[a], and Ju Chen[a]
[a]School of Medicine, University of California, San Diego, La Jolla, CA 92093-0613; [b]Randall Division for Cell and Molecular Biophysics and Cardiovascular Division, King's College London BHF Centre of Research Excellence, London SE1 1UL, United Kingdom

ABSTRACT **Protein turnover through cullin-3 is tightly regulated by posttranslational modifications, the COP9 signalosome, and BTB/POZ-domain proteins that link cullin-3 to specific substrates for ubiquitylation. In this paper, we report how potassium channel tetramerization domain containing 6 (KCTD6) represents a novel substrate adaptor for cullin-3, effectively regulating protein levels of the muscle small ankyrin-1 isoform 5 (sAnk1.5). Binding of sAnk1.5 to KCTD6, and its subsequent turnover is regulated through posttranslational modification by nedd8, ubiquitin, and acetylation of C-terminal lysine residues. The presence of the sAnk1.5 binding partner obscurin, and mutation of lysine residues increased sAnk1.5 protein levels, as did knockdown of KCTD6 in cardiomyocytes. Obscurin knockout muscle displayed reduced sAnk1.5 levels and mislocalization of the sAnk1.5/KCTD6 complex. Scaffolding functions of obscurin may therefore prevent activation of the cullin-mediated protein degradation machinery and ubiquitylation of sAnk1.5 through sequestration of sAnk1.5/KCTD6 at the sarcomeric M-band, away from the Z-disk–associated cullin-3. The interaction of KCTD6 with ankyrin-1 may have implications beyond muscle for hereditary spherocytosis, as KCTD6 is also present in erythrocytes, and erythrocyte ankyrin isoforms contain its mapped minimal binding site.**

Monitoring Editor
William P. Tansey
Vanderbilt University

Received: Jan 24, 2012
Revised: Apr 5, 2012
Accepted: Apr 27, 2012

INTRODUCTION

The exact mechanism underlying the simultaneous degradation and synthesis of myofibrils in actively working myocytes remains a mystery in muscle biology. Muscle cells contain up to four proteolytic systems that enable them to achieve coordinated protein turnover (Martinez-Vicente *et al.*, 2005; Su and Wang, 2010): the caspase and calpain systems of partially muscle-specific proteases; the ubiquitin proteasome system (UPS), which degrades polyubiquitylated proteins via the 26S proteasome; and the autophagy system, which removes proteins by inclusion in autophagic/lysosomal vesicles. These systems do not necessarily operate in isolation, as there is increasing evidence of cross-talk between autophagy and the UPS (Bjorkoy *et al.*, 2009). The UPS consists of two parts: an enzymatic cascade attaching ubiquitin to substrates intended for degradation and the proteasome complex, which facilitates proteolytic cleavage of polyubiquitylated substrates. Specific substrate recognition is achieved by dedicated ubiquitin E3 ligases. More than 100 such E3-enzymes are described, some of which (e.g., the muscle-specific ring-finger [MuRF] family) are specific for striated muscle. Cullin proteins are another set of ubiquitin E3 ligases that are ubiquitously expressed. In contrast to other E3 ligases, cullins do not bind their substrate directly, but rely on an array of adaptor proteins, such as the muscle-specific atrogin-1 (MAFbx/FBXO32; Gomes *et al.*, 2001). Besides F-box–containing proteins, substrate adaptors containing BTB/POZ domains are also considered another class of linker proteins.

This article was published online ahead of print in MBoC in Press (http://www.molbiolcell.org/cgi/doi/10.1091/mbc.E12-01-0052) on May 9, 2012.

Address correspondence to: Ju Chen (juchen@ucsd.edu) or Stephan Lange (slange@ucsd.edu).

Abbreviations used: BSA, bovine serum albumin; BTB, broad-complex, tramtrack and brick-a-brac; CHX, cycloheximide; DAPI, 4′,6-diamidino-2-phenylindole; DH, Dbl homology domain; DIA, diaphragm; FBXO32, F-box protein 32; GFP, green fluorescent protein; GST, glutathione *S*-transferase; HA, hemagglutinin epitope tag; HDAC, histone deacetylase; KCTD6, potassium channel tetramerization domain containing 6; MAFbx, muscle atrophy F-box; MuRF, muscle-specific ring-finger; NCBI, National Center for Biotechnology Information; NRC, neonatal rat cardiomyocytes; OBD-2, obscurin binding domain 2; Obsl1, obscurin-like 1; PBS, phosphate-buffered saline; PFA, paraformaldehyde; PH, pleckstrin homology domain; POZ, pox virus and zinc finger; RNAi, RNA interference; sAnk1.5, small ankyrin-1 isoform 5; SAP, shrimp alkaline phosphatase; SH3, SRC homology 3 domain; siRNA, small interfering RNA; SPEG/APEG, striated muscle preferentially expressed protein kinase; SR, sarcoplasmic reticulum; TSA, trichostatin A; UPS, ubiquitin proteasome system; Xgal, 5-bromo-4-chloro-indolyl-β-D-galactopyranoside; YFP, yellow fluorescent protein.

One recently described BTB/POZ domain–containing protein family that may act as cullin-3 substrate linkers are the KCTD proteins. KCTD proteins were named after their N-terminal BTB/POZ domain, which has high homology with tetramerization domains of potassium channels. Among the 22 KCTD proteins in humans, KCTD5 (Bayon *et al.*, 2008), KCTD13/BACURD1, as well as KCTD13's paralogue TNFAIP1 (BACURD2; Chen *et al.*, 2009) have been demonstrated to interact directly with cullin-3 and mediate substrate recognition for subsequent ubiquitylation. Specific substrates for the KCTD–cullin complex include the small GTPase RhoA (Chen *et al.*, 2009) and, putatively, the Golgi-associated GRASP55 (Dementieva *et al.*, 2009).

It is documented that muscle-specific E3 ligases can bind to sarcomeric proteins such as titin (Spencer *et al.*, 2000; Centner *et al.*, 2001; McElhinny *et al.*, 2002; Witt *et al.*, 2005; Mrosek *et al.*, 2007; Muller *et al.*, 2007) and participate in sarcomerogenesis and myofibrillar maintenance (Lange *et al.*, 2005b; Perera *et al.*, 2011). Conversely, it is yet to be determined whether ubiquitous E3 ligases, such as cullin proteins could also have important roles in muscle development and function. Intriguingly, cardiac-specific ablation of CSN8, a COP9-signalosome subunit involved in the regulation of cullin activity, leads to a dilated cardiomyopathy phenotype (Su *et al.*, 2010), while cullin-7/p193 overexpression improves cardiac function (Nakajima *et al.*, 2004; Hassink *et al.*, 2009). Moreover, the strong sarcomeric association of the cullin-1 substrate linker atrogin-1 with components of the sarcomeric Z-disk (Li *et al.*, 2004) and the M-band association of CSN5 in *Caenorhabditis elegans* muscle (Miller *et al.*, 2009) highlight the importance of this class of E3 ligases for striated muscles.

Like titin, members of the obscurin protein family are thought to be important for sarcomere assembly and maintenance. Composed mainly of immunoglobulin-like and fibronectin type-III domains, the obscurin protein family consists of three members: obscurin (Bang *et al.*, 2001; Young *et al.*, 2001), obscurin-like 1 (Obsl1; Geisler *et al.*, 2007; Fukuzawa *et al.*, 2008), and striated muscle preferentially expressed protein kinase (SPEG/APEG; Hsieh *et al.*, 2000; Liu *et al.*, 2009). In contrast to Obsl1, obscurin and SPEG/APEG contain additional protein kinase domains, RhoGEF domains, or an IQ-motif, hinting at a role for both proteins in muscle-specific signaling (Young *et al.*, 2001; Bowman *et al.*, 2008; Ford-Speelman *et al.*, 2009). One of the best-characterized functions of the obscurin-A C-terminus is its interaction with small ankyrin-1 isoform 5 (sAnk1.5; Bagnato *et al.*, 2003; Kontrogianni-Konstantopoulos *et al.*, 2003). This muscle-specific isoform of ankyrin-1 lacks all characteristic domains associated with ankyrin proteins: N-terminal ankyrin repeats, a spectrin-binding domain, and the C-terminal death domain, but includes in its N-terminus a unique transmembrane domain that integrates into the sarcoplasmic reticulum (SR) of cross-striated muscle cells (Gallagher and Forget, 1998; Porter *et al.*, 2005). We previously showed that ablation of obscurin leads to reduction of sAnk1.5 protein levels, its mislocalization to the sarcomeric Z-disk/I-band region, and dramatically altered SR architecture (Lange *et al.*, 2009).

More recently it has emerged that mammalian obscurin proteins or the *C. elegans* homologue UNC-89 associate either indirectly (Hanson *et al.*, 2009; Huber *et al.*, 2009) or directly (Litterman *et al.*, 2011; G. Benian, personal communication) with cullins, and putatively regulate cullin-mediated protein turnover (Miller *et al.*, 2006, 2009).

In this study, we set out to further investigate why sAnk1.5 protein levels were reduced in muscles of obscurin knockout animals by studying novel sAnk1.5 interactions. We show that sAnk1.5 turnover is regulated by posttranslational modification, presence of obscurin, and tissue-specific interaction with a novel partner—potassium channel tetramerization domain containing 6 (KCTD6). We characterize the biological functions of KCTD6 as a specific linker for cullin-3–dependent protein turnover, as well as its oligomerization and interaction with sAnk1.5.

The presence of the KCTD6 binding site in erythrocyte isoforms of ankyrin-1 and detection of KCTD6 in purified red blood cells indicate that this interaction may have implications beyond striated muscles. Indeed, pathological mutations that result in truncated ankyrin-1 lacking the KCTD6 binding site may suggest a role for this complex in the development of hereditary spherocytosis.

RESULTS

sAnk1.5 interacts with KCTD6 in striated muscle

In search for interaction partners for the muscle-specific isoform sAnk1.5 of ankyrin 1, we performed a yeast two-hybrid screen using a human cardiac cDNA library as bait and the cytoplasmic part of sAnk1.5 as prey. Out of 30 clones, four correctly identified the obscurin C-terminus as an sAnk1.5 binding partner, indicating the successful implementation of the screening method. Eight clones encoded for the N-terminus of KCTD6, a novel interaction partner for sAnk1.5 (Table 1). Verification of the interaction by forced yeast two-hybrid assays (Figure 1A) and coimmunoprecipitations (Figure 1C) indicated that the minimal binding sites for the interaction reside in the N-terminal BTB/POZ domain of KCTD6 (Figure 1D), as well as within a region of sAnk1.5 encompassing the obscurin binding domain 2 (OBD-2; Figure 1B). Failure to demonstrate binding using bacterially expressed glutathione *S*-transferase (GST)-tagged ankyrin (residues 29–155) in pulldowns (Supplemental Figure S1A) or full-length KCTD6 derived from nonmyogenic cells (Figure 1C) suggested that the interaction is dependent on tissue-specific posttranslational modifications of ankyrin and/or KCTD6.

We reported previously that ankyrin undergoes posttranslational modification by ubiquitin and/or nedd8 (Lange *et al.*, 2009). However, Lys-R mutants that lack the modification of sAnk1.5 by ubiquitin-like modifiers (Lange *et al.*, 2009), as well as Cys/Gly mutants that cannot form ankyrin dimers via cysteine bridges (Porter *et al.*, 2005), retain their ability to interact with KCTD6 (Figure S1C), suggesting another form of posttranslational modification necessary for the KCTD6/sAnk1.5 complex formation. To identify whether phosphorylation of sAnk1.5 or KCTD6 triggers the interaction, we performed mutational analysis of serine or threonine residues in sAnk1.5 and

Clone number	NCBI accession number	Protein
1	NM_052843.2	Obscurin
3	NM_153331	KCTD6
5	NM_153331	KCTD6
12	NM_153331	KCTD6
16	NM_153331	KCTD6
17	NM_052843.2	Obscurin
19	NM_153331	KCTD6
20	NM_153331	KCTD6
21	NM_153331	KCTD6
23	NM_052843.2	Obscurin
24	NM_153331	KCTD6
26	NM_052843.2	Obscurin

TABLE 1: sAnk1.5 cytoplasmic part yeast two-hybrid results.

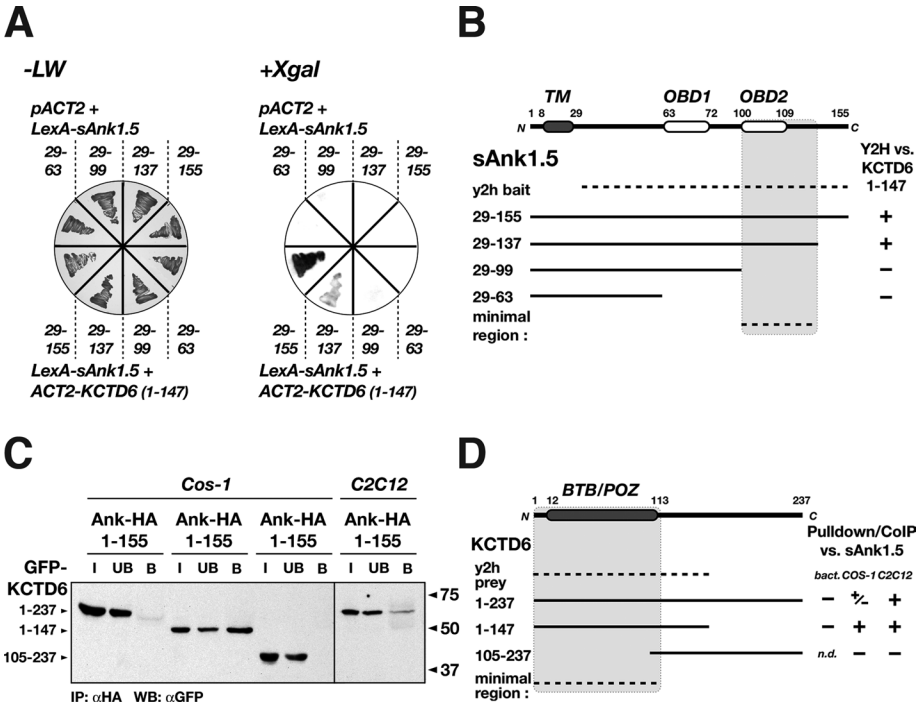

FIGURE 1: sAnk1.5 interacts with KCTD6 in a tissue-specific manner. (A) Forced yeast two-hybrid identified a region including OBD-2 as minimal binding site for KCTD6. Yeast transformed with either empty pACT2 vector or pACT2-KCTD6 (residues 1–147) together with pLexA-sAnk1.5 constructs expressing small ankyrin regions 29–155, 29–137, 29–99, or 29–63 were grown on SD-LW minimal medium (left). Xgal filter assay (right) indicated a region within sAnk1.5 residues 100–137 as a minimal binding site for sAnk1.5 interaction with KCTD6. (B) Schematic representation of sAnk1.5 domain structure and mapped KCTD6 minimal-binding site. TM, transmembrane domain; OBD, obscurin binding domain. All residues are for human sAnk1.5 (NCBI accession number: NP_065211). (C) Coimmunoprecipitation of either full-length GFP-tagged KCTD6, KCTD6 N-terminus (residues 1–147), or C-terminus (residues 105–237) with HA-tagged sAnk1.5 using cell lysates from transfected Cos-1 or differentiated C2C12 cells (day 7). Full-length KCTD6 displays binding to sAnk1.5 only in lysates from differentiated C2C12 cells, whereas proteins isolated from transfected Cos-1 cells demonstrated only interaction of KCTD6 N-terminus with sAnk1.5. I, input; UB, unbound; B, bound fractions. (D) Schematic representation of KCTD6 domain structure and minimal sAnk1.5 binding site. The minimal binding site to sAnk1.5 encompasses the N-terminal BTB/POZ domain in KCTD6. Results for GST-pulldown assays (Figure S1A), coimmunoprecipitations from transfected Cos-1 or C2C12 cell lysates (C) demonstrate the muscle-specific interaction of sAnk1.5 with full-length KCTD6. All residues are for human KCTD6 (NCBI accession number: NP_699162).

KCTD6. Mutation of Ser-113, Ser-114, and Ser-129 in sAnk1.5 to either alanine or aspartic acid did not alter the interaction of sAnk1.5 with KCTD6 (Figure 2A), nor did mutation of Ser-130, Ser-155, Ser-214, or Thr-199 in KCTD6 (unpublished observations). Moreover, staurosporine and/or phosphatase treatment of KCTD6 and sAnk1.5 from C2C12 cells did not inhibit binding (Figure S1B). Therefore phosphorylation of sAnk1.5 and/or KCTD6 in the investigated residues does not trigger their interaction. Intriguingly, mutation of Lys-101 in sAnk1.5's obscurin binding domain 2 (OBD-2) to glutamic acid, which completely abrogates obscurin binding (Borzok *et al.*, 2007), could decrease, but not inhibit, formation of the KCTD6/sAnk1.5 complex (Figure 2, A and B). The intact interaction of KCTD6 with the Lys-101E sAnk1.5 mutant indicates further that sAnk1.5 may bind obscurin and KCTD6 simultaneously. Indeed, the localization of KCTD6 and sAnk1.5 at the level of the sarcomeric M-band in heart and skeletal muscle (Figure 2, C–E) supports the formation of a ternary obscurin–sAnk1.5–KCTD6 complex, as does coimmunoprecipitation of KCTD6 N-terminus (1–147) with sAnk1.5 and the obscurin-A C-terminus (Figure S1C). Colocalization of KCTD6 N-terminus (1–147) and sAnk1.5 in transfected Cos-1 cells (Figure S1D) further supports binding within cells. KCTD21, which is the closest paralogue to KCTD6 (Bayon *et al.*, 2008), and KCTD5 demonstrated no interaction with sAnk1.5, highlighting the specificity of the ankyrin–KCTD6 interaction (unpublished observations).

Binding of sAnk1.5 to KCTD6 is promoted by acetylation

Recently, KCTD6 has been implicated in histone deacetylase (HDAC) signaling and deacetylase turnover (De Smaele *et al.*, 2011). We investigated whether acetylation of sAnk1.5 may promote interaction of full-length KCTD6 with sAnk1.5 in nonmuscle cells. Treatment of Cos-1 cells with HDAC-inhibitor TSA allowed binding of sAnk1.5 to KCTD6, whereas KCTD6 assayed from untreated Cos-1 cells showed no interaction (Figure 2B). Moreover, immunoprecipitation of proteins containing acetylated lysine residues suggested acetylation of sAnk1.5 in trichostatin A (TSA)-treated Cos-1 cells, as compared with lower levels of acetylated sAnk1.5 from untreated cells (Figure 2F, left side of right panel). In comparison, full-length KCTD6 showed no appreciable lysine acetylation, even upon TSA treatment of Cos-1 cells (Figure S2A, right panel), suggesting that acetylation of sAnk1.5 may trigger binding of the two proteins. To identify acetylated regions within sAnk1.5, we transfected Cos-1 cells with either full-length sAnk1.5, or C-terminal truncation constructs expressing residues 1–137, 1–99, 1–63, and a mutated 1–63 sAnk1.5 version that replaces lysine residues 38 and 46 with arginine (Figure 2F, right side of right panel). High levels of acetylated ankyrin were observed with the full-length sAnk1.5, whereas truncation of sAnk1.5 C-terminus to residue 137 or 99 resulted in decreased or abrogated acetylation of the protein, respectively. We then investigated whether increased binding of acetylated sAnk1.5 to KCTD6 can be automatically correlated with increased sAnk1.5 protein turnover. Surprisingly, HDAC inhibition by TSA did not alter protein turnover of sAnk1.5 in transfected Cos-1 cells (Figure S2B), indicating that ubiquitylation by E3 ligases and/or degradation of ubiquitylated proteins by the proteasome may be further regulated by other cofactors. Taken together, these results indicate that acetylation of the sAnk1.5 C-terminal lysine residues (Figure 3F) may promote interaction with KCTD6. Increased binding of sAnk1.5 to KCTD6, however, does not automatically correlate with increased sAnk1.5 protein turnover.

KCTD6 and sAnk1.5 associate with ubiquitin and ubiquitin-like modifiers

Ankyrins are subjected to the E3-ligase activity of spectrins, their interaction partners (Chang *et al.*, 2004; Hsu and Goodman, 2005). We previously demonstrated that sAnk1.5 is modified by ubiquitin and nedd8 (Lange *et al.*, 2009), however, it lacks all the necessary

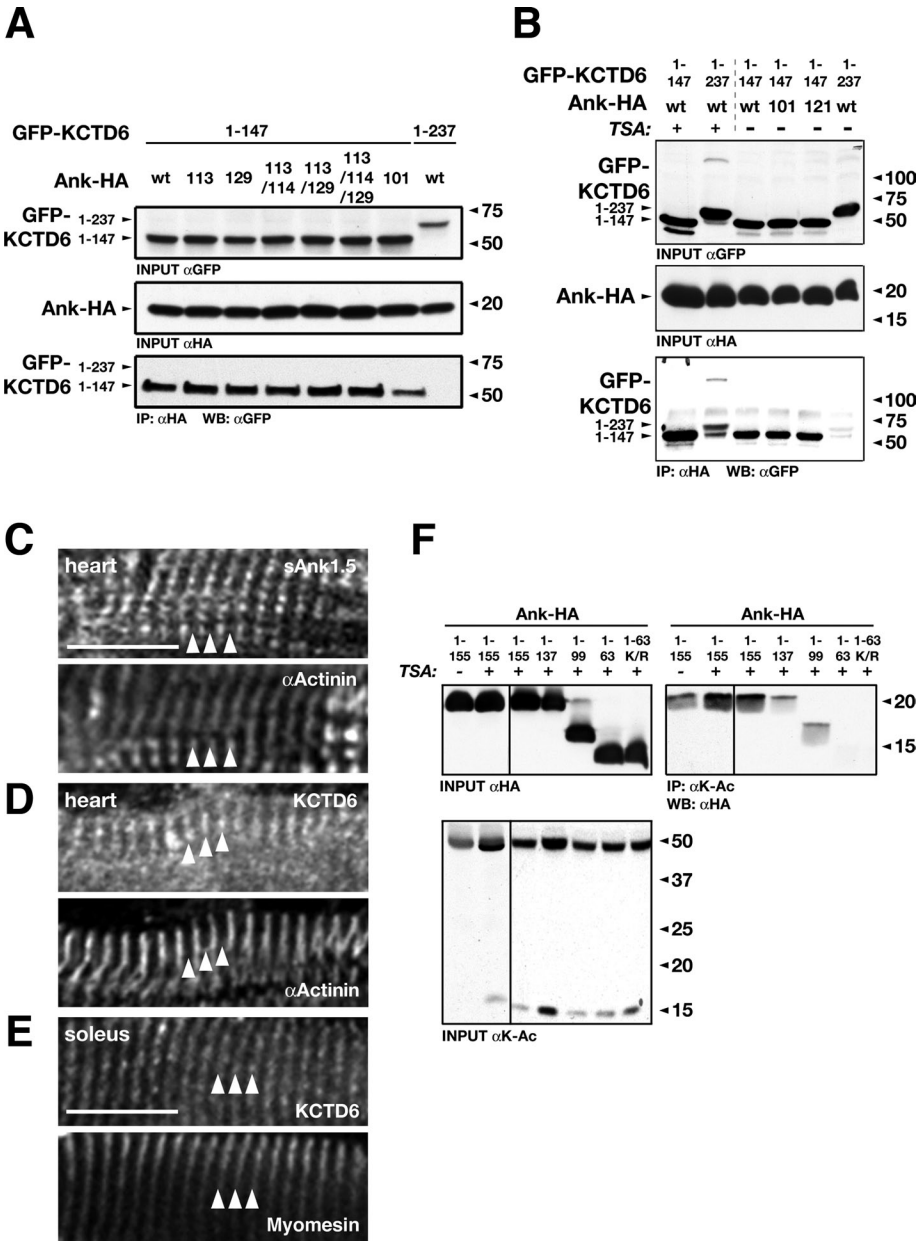

FIGURE 2: Posttranslational modification of sAnk1.5 affects its interaction with KCTD6. (A) Mutational analysis of putative serine phosphorylation sites and conserved lysine in minimal KCTD6 binding site of sAnk1.5 (residues 100–137). Coimmunoprecipitation of transfected Cos-1 cells expressing GFP-tagged KCTD6 N-terminus with either HA-tagged sAnk1.5 wild-type, Ser-113A, Ser-129A, Ser-113/114A, Ser-113/129A, Ser-113/114/129A, or Lys-101E (Borzok *et al.*, 2007) mutants displayed weaker, but not abrogated, binding of KCTD6 to sAnk1.5 Ser-101E mutant. Full-length KCTD6 shows no binding to sAnk1.5 in Cos-1 cells. (B) HDAC inhibition by TSA triggers binding of sAnk1.5 with full-length KCTD6 in nonmuscle cells. Binding of wild-type and mutant sAnk1.5 (Lys-101E, Glu-121K) to either full-length of C-terminally truncated KCTD6 (residues 1–147) from Cos-1 cells was assessed in absence or presence of 0.5 μg/ml TSA. Mutation of either Lys-101E or Glu-121K did not alter interaction of sAnk1.5 to C-terminally truncated KCTD6. Full-length KCTD6 isolated from COS-1 cells only interacted with sAnk1.5 after incubation of cells with TSA.
(C to E) Subcellular localization of endogenous sAnk1.5 (C), KCTD6 (D and E) in heart (C and D) or skeletal muscle cells (E) shows that both proteins localize at the M-band in wild-type cross-striated muscles. (C to E) Scale bar: 10 μm. (F) Acetylation of sAnk1.5 C-terminus. Inhibition of HDAC by TSA leads to increased acetylation of sAnk1.5 as demonstrated by coimmunoprecipitation using an acetyl-lysine antibody (K-Ac; right). Truncation of the sAnk1.5 C-terminus decreases (residues 1–137) or abolishes acetylation (residues 1–63; residues 1–63 Lys-38/46R double mutant).

binding sites for spectrin proteins. Because neddylation of a substrate protein has been reported to enhance its subsequent ubiquitylation (Pan *et al.*, 2004; Oved *et al.*, 2006), we investigated the temporal order and spatial relationship between sAnk1.5 and nedd8 or ubiquitin. Using the protein complementation assay (split–fluorescent protein system), we observed that in the absence of the proteasome inhibitor MG132, only sAnk1.5 modified by nedd8 can be detected (Figure 3A). Detectable association of sAnk1.5 with ubiquitin could only be demonstrated after treatment of cells with MG132 (Figure 3B). These results indicate that ubiquitylated sAnk1.5 is too short-lived to allow detectable complementation of the fluorescent protein, whereas neddylated sAnk1.5 appears more stable, as evidenced by readily observable yellow fluorescent protein (YFP) fluorescence (Figure 3A, top panel). Sumo1, another ubiquitin-like modifier, demonstrated no association with sAnk1.5 (Figure S2C). These results are congruent with previous data, confirming that neddylated sAnk1.5 exhibits lower molecular weights compared with polyubiquitylated sAnk1.5 and that sAnk1.5 is not sumoylated (Lange *et al.*, 2009).

To investigate which lysine residues in sAnk1.5 allow attachment of ubiquitin, we investigated the rate of sAnk1.5 protein degradation using the ribosome inhibitor cycloheximide (CHX). We determined that sAnk1.5 half-life in transfected Cos-1 cells is ~6 h (Figure 3D, black bars), which is comparable with the turnover of endogenous sAnk1.5 measured in differentiated C2C12 cells (Figure 3C). Using wild-type sAnk1.5 and Lys-38R, Lys-46R, Lys-73R, Lys-105R, and Lys-38/73R sAnk1.5 mutants (Figure 3, D–F), we could demonstrate that sAnk1.5 mutated at lysine residues Lys-38 and K73 exhibits significantly increased protein levels after 6 h of CHX treatment, indicating impairment of sAnk1.5 turnover in these mutants. We also studied whether the presence of the obscurin-A C-terminus exerts an influence on sAnk1.5 turnover, but found no noticeable difference (Figure 3E, black bars). Analysis of Lys-38R, Lys-73R, Lys-105R, and Lys-38/73R mutants, however, showed significantly increased sAnk1.5 levels when coexpressed with obscurin. Specifically, the decreased protein turnover for the Lys-38R mutant coexpressed with obscurin indicates that some lysine residues located in OBD-1 and -2 of ankyrin may be engaged in binding obscurin and are therefore inaccessible for ubiquitylation.

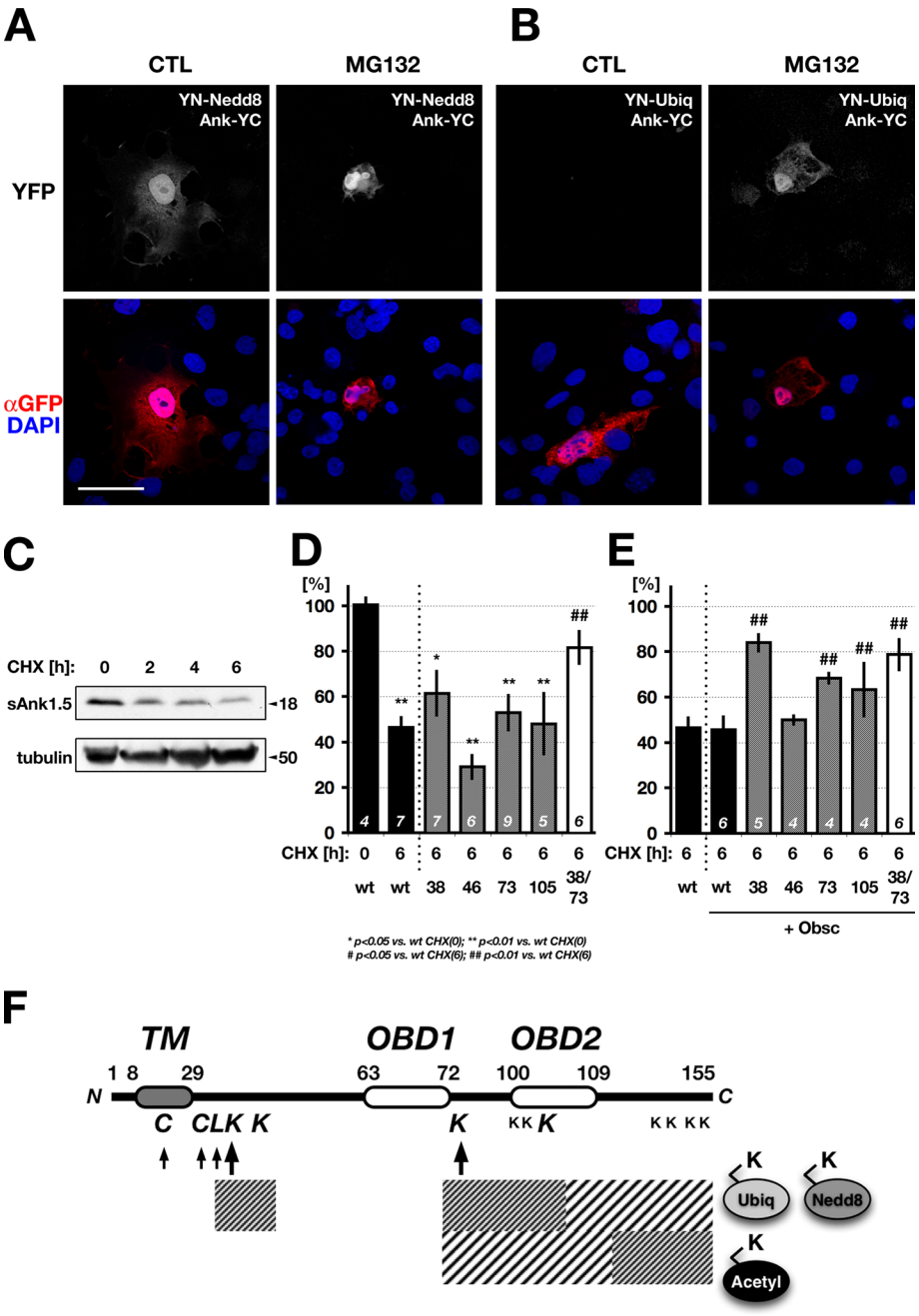

FIGURE 3: sAnk1.5 is modified by nedd8 and ubiquitin. Identification of lysine residues important for protein turnover. (A) Protein complementation assay using YFP (split–fluorescent protein assay) demonstrated neddylation of sAnk1.5 in Cos-1 cells. Cos-1 cells transfected with N-terminal YFP-tagged (YN; Zou *et al.*, 2006) nedd8 and C-terminal YFP-tagged (YC) sAnk1.5 (bottom, GFP antibody staining red in overlay) display close association/modification of sAnk1.5 by nedd8 as evidenced by complementation of YFP and restoration of endogenous fluorescence (top). Note that the putative neddylation of sAnk1.5 is readily visible without MG132 treatment. (B) Protein complementation assay as in (A) using YN-ubiquitin and sAnk1.5-YC demonstrated visible modification of sAnk1.5 by ubiquitin only in MG132 treated Cos-1 cells (top). Untreated Cos-1 cells show no detectable ubiquitylation of sAnk1.5, despite expression of constructs (bottom, GFP-antibody red in overlay, DAPI blue in overlay). Scale bar: 20 μm. (C) Analysis of endogenous sAnk1.5 protein degradation in differentiated C2C12 cells using ribosome inhibitor CHX, shows an apparent protein half-life of ~5 h, comparable with transfected sAnk1.5 in Cos-1 cells (see D). Loading control: β-tubulin. (D) CHX treatment of COS-1 cells transfected with wild-type or mutant sAnk1.5 indicates Lys-38 and Lys-73 as important for ubiquitylation/degradation. Cos-1 cells transfected with HA-tagged wild-type, Lys-38R, Lys-46R, Lys-73R, Lys-105R or Lys-38/73R sAnk1.5 were treated with 10 μg/ml CHX for 6 h. Densitometric quantification of wild-type sAnk1.5 levels indicated a protein half-life of ~6 h (black bars). Comparison of lysine mutants with the wild-type protein after 6 h of CHX treatment displayed a slight increase of sAnk1.5 for Lys-38R and Lys-73R mutants. The Lys-38/73R double mutant showed significantly increased protein amount (white bar), when compared with wild-type sAnk1.5 after 6 h of treatment. (E) Presence of obscurin C-terminus influences sAnk1.5 degradation. Cos-1 cells transfected with wild-type, Lys-38R, Lys-46R, Lys-73R, Lys-105R or Lys-38/73R sAnk1.5 with or without obscurin C-terminus encompassing the ankyrin binding site (Bagnato *et al.*, 2003; Kontrogianni-Konstantopoulos *et al.*, 2003) were treated with CHX for 6 h. Whereas wild-type sAnk1.5 showed no change in its degradation with or without coexpression of obscurin (black bars), Lys-38R, Lys-73R, Lys-105R and Lys-38/73R mutants show significantly increased sAnk1.5 levels after 6 h of CHX treatment, when coexpressed with obscurin. Similarity of Lys-38R mutant sAnk1.5 levels in presence of obscurin, with amounts of sAnk1.5 Lys-38/73R double mutant (in D) indicate that either Lys-73R mutation, or binding of Lys-73 with obscurin are beneficial for sAnk1.5 protein half-life. (D and E) p values, n values (bottom of each graph), and SEM are displayed. (F) Representation of sAnk1.5 domain layout and posttranslational modification by ubiquitin, nedd8, and acetylation. Lysines in sAnk1.5 and regions responsible for posttranslational modification are indicated (dark shaded = high likelihood of modification). Lysines mutated for protein turnover investigations displayed in bigger letters. Arrows indicate residues influencing turnover.

Ankyrin has been shown to form oligomeric complexes (Porter *et al.*, 2005), presumably through disulfide bridges at the Cys-22/Cys-34 residues. Analysis of the sAnk1.5 secondary structure (Figure S2D) indicated the presence of a helical region in the cytoplasmic part of sAnk1.5 (residues 29–47) immediately following the helical transmembrane domain. Intriguingly, residues Leu-33, Leu-37, Ile-40, and Leu-44 form a hydrophobic pocket in the pinwheel view (Figure S2F), which may help to promote ankyrin oligomerization. To investigate whether oligomerization of sAnk1.5 may play a role in its turnover, we assessed the cysteine–glycine mutant Cys-22G/Cys-34G, the Leu-44R mutant, and the Cys-22G/Cys-34G/Leu-44R triple mutant. Comparison of wild-type sAnk1.5 after 6 h of CHX treatment with either of these mutants showed that abrogation of disulfide-bridge formation resulted in increased protein turnover, whereas additional mutation of Leu-44R in the Cys-22G/Cys-34G/Leu-44R mutant significantly decreased sAnk1.5 protein degradation (Figure S2E).

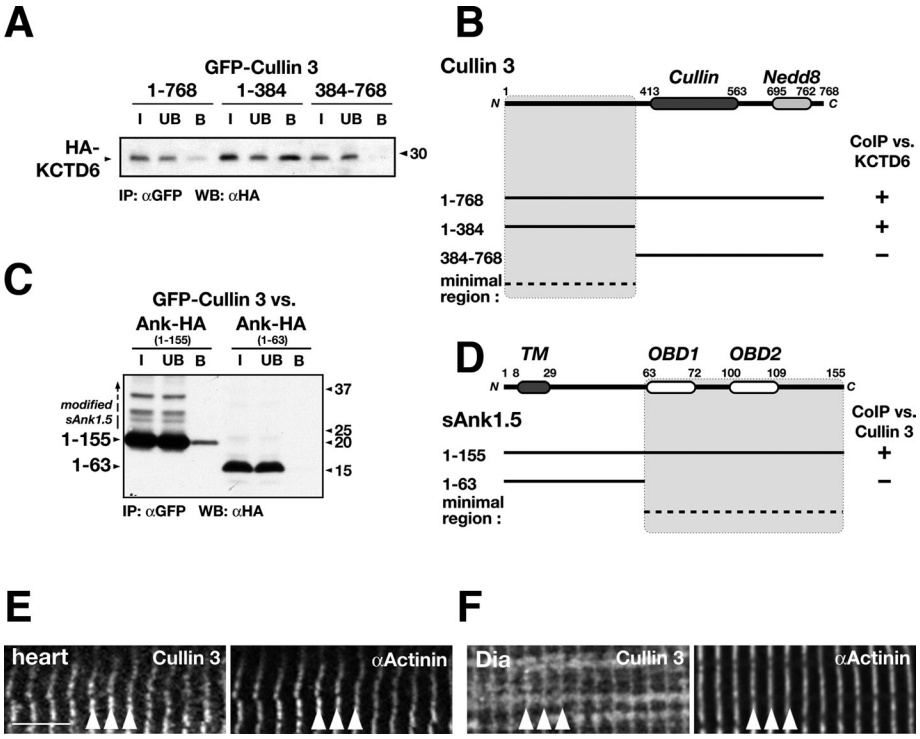

FIGURE 4: Association of sAnk1.5 and KCTD6 with E3 ligase cullin-3. (A) KCTD6 associates with the unstructured cullin-3 N-terminus. Coimmunoprecipitation of HA-tagged KCTD6 with GFP-tagged full-length cullin-3, cullin-3 N-terminus (residues 1–384), or cullin-3 C-terminus (residues 384–768) shows binding of KCTD6 to the N-terminal region of cullin-3. (B) Schematic representation of cullin-3 domain structure and minimal KCTD6 binding site as determined in (A). Cullin ligase domain and Nedd8 modification site in cullin-3 are indicated. Residue numbers according to human cullin-3 (NCBI accession number: NP_003581). (C) Coimmunoprecipitation of full-length or sAnk1.5 N-terminus (residues 1–63) demonstrates association of cullin-3 with full-length unmodified sAnk1.5, but not of the sAnk1.5 N-terminus. (A and C) I, input; UB, unbound; B, bound fractions. (D) Schematic representation of ankyrin domain structure and protein region required for association of sAnk1.5 with cullin-3, as demonstrated in (C). (E and F) Immunofluorescence of cardiac (E) and skeletal muscle (F, Dia) display localization of cullin-3 to the sarcomeric Z-disk (arrowheads) as validated by colocalization with sarcomeric α-actinin. Scale bar: 6 μm.

In summary, we observed that sAnk1.5 protein turnover depends on the availability of Lys-38 and Lys-73 for ubiquitylation (Figure 3F, big arrows), the presence of the ankyrin binding partner obscurin, and the oligomerization state of the protein.

We also considered whether KCTD6 is involved in the neddylation/ubiquitylation process of its interaction partner sAnk1.5, and whether KCTD6 itself may be subject to neddylation/ubiquitylation by using the protein complementation assay. Although KCTD6 is found in proximity to nedd8 within cells (Figure S2G), it is not post-translationally altered by ubiquitin or ubiquitin-like modifiers in baseline conditions, as evidenced by the absence of higher-molecular-weight bands representing modified KCTD6 in immunoblots (Figure S3A). Similar to sAnk1.5, KCTD6 is only associated with ubiquitin after MG132 treatment (Figure S2H), and not with Sumo1 (Figure S2I). These data indicate a role for KCTD6 in neddylation and ubiquitylation of substrate proteins such as sAnk1.5, without KCTD6 itself being subjected to modification by nedd8.

KCTD6 mediates sAnk1.5 association to cullin-3

BTB/POZ domain–containing proteins act as scaffolding/adaptor proteins in a variety of complexes. A prominent example is the cullin-3 E3 ligase that requires BTB/POZ domain–containing proteins to link it to its substrates (Bosu and Kipreos, 2008). It has recently emerged that two KCTD family members, KCTD5 and KCTD13 (BACURD1), interact with and may be targets of cullin-3 (Bayon *et al.*, 2008; Chen *et al.*, 2009). We therefore asked whether association of KCTD proteins with cullin-3 is a general hallmark of this protein family, and whether KCTD6 is a putative binding partner of cullin-3.

Coimmunoprecipitation assays confirmed that KCTD6 interacts with the unstructured cullin-3 N-terminus (Figure 4, A and B), as recently reported (De Smaele *et al.*, 2011). This feature is reminiscent of the interaction of KCTD5 with cullin-3, whereby the BTB domain of KCTD5 also interacts with the N-terminal half of cullin-3 (Bayon *et al.*, 2008). However, in contrast with sAnk1.5 (Lange *et al.*, 2009), KCTD6 did not undergo neddylation (Figure S3A). Next we analyzed whether sAnk1.5 itself is associated with cullin-3. Coimmunoprecipitation of sAnk1.5 with cullin-3 demonstrates a linkage between the two proteins (Figure 4, C and D) putatively mediated by endogenous KCTD proteins. Intriguingly, only full-length, but not modified or truncated, sAnk1.5 (Figure 4C) could be precipitated by cullin-3.

Endogenous cullin-3 in cardiomyocytes and skeletal muscle cells localizes at the sarcomeric Z-disk (Figure 4, E and F). However, since cullin action is enzymatic, minute levels of cullin-3 should be sufficient to mediate ubiquitylation of target proteins outside the Z-disk region. Additionally, we observed that cullin-3 colocalizes with KCTD6 (Figure S3, B, D, and E), and sAnk1.5 in Cos-1 cells (Figure S3C).

KCTD6 is up-regulated during muscle development

Nedd8 was reported to be down-regulated during embryonic development (Kamitani *et al.*, 1997). To gain insight into the precise spatial and temporal expression of nedd8, KCTD6, cullin, and COP9 signalosome–associated proteins, and their relevance for muscle development and function, we studied their expression levels and localization in various tissues during development.

KCTD6 is expressed in a broad range of tissues. The highest expression was found in the liver, for which a 30-kDa band was observed (Figure 5A, top KCTD6 panel). Heart, kidney, and smooth muscle (stomach) displayed a 25-kDa immunopositive band, indicating two distinct KCTD6 moieties. Longer exposure revealed the 30-kDa band to be almost ubiquitous (Figure 5A, bottom KCTD6 panel). Cullin-3 (Figure 5A) and nedd8 (Figure S4A) were also detected in all investigated tissues. To address whether cullin-mediated protein turnover was important for sarcomerogenesis, we explored the expression profile of KCTD6, cullin-3, the cullin-associated protein Skp1, and CSN5 as a representative of the COP9 signalosome during postnatal heart growth and C2C12 differentiation.

Expression levels of KCTD6 and sAnk1.5 increased during postnatal heart development and C2C12 myotube formation (Figure 5, B and C), comparable with the developmental regulation of Skp1 and sarcomeric myosin (Figures 5C and S4B). Up-regulation of

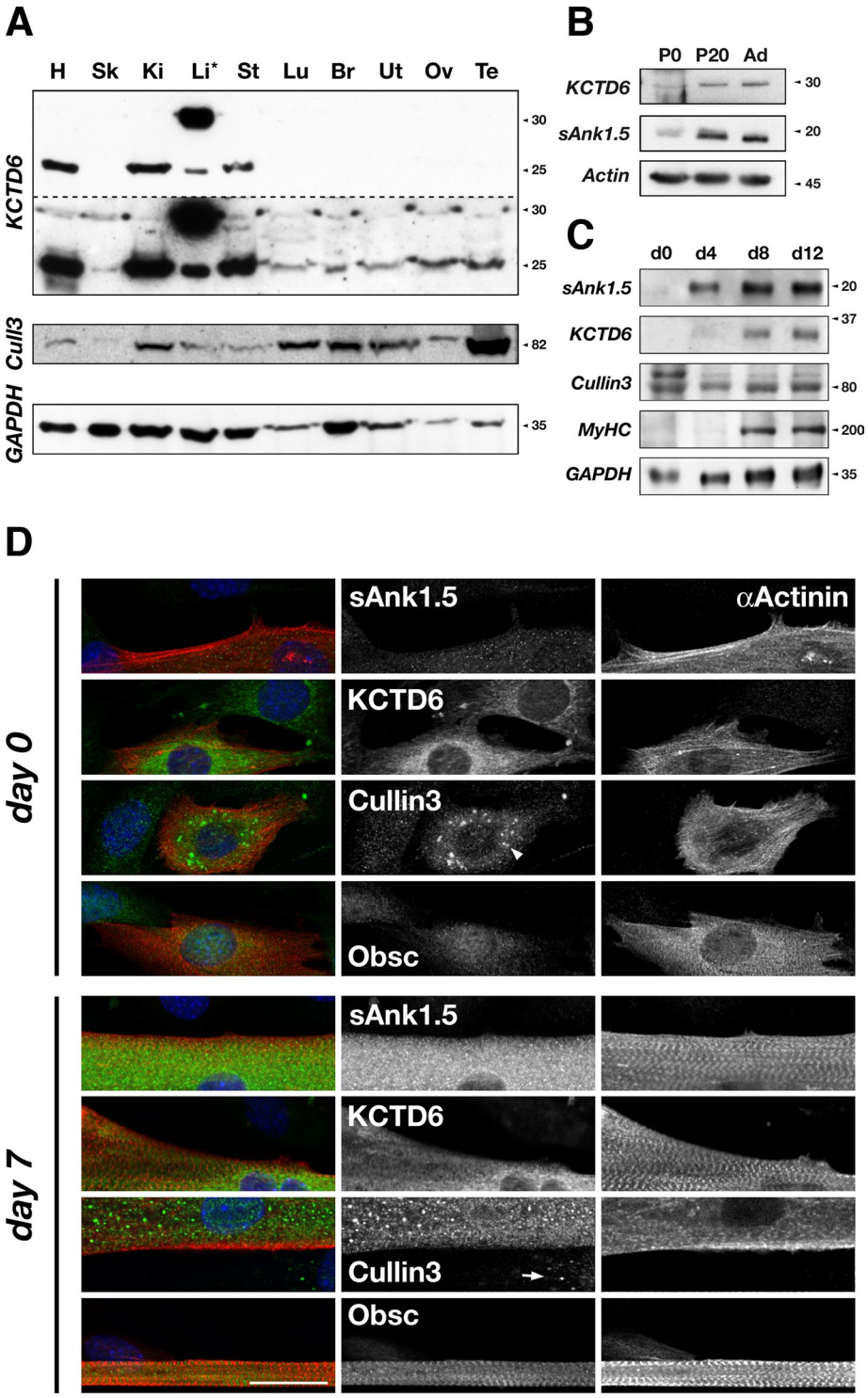

FIGURE 5: Analysis of KCTD6 developmental and tissue-specific expression pattern. (A) Analysis of endogenous KCTD6 and cullin-3 protein levels in various mouse tissues. High levels of KCTD6 were found in heart (H), kidney (Ki), liver (Li), and stomach (St; top, KCTD6 blot). Ubiquitous low expression was also found in all other analyzed tissues, namely skeletal muscle (Sk), lung (Lu), brain (Br), uterus (Ut), ovaries (Ov), and testes (Te). Note that the KCTD6 antibody cross-reacts with bands at approximately 30 kDa and 25 kDa, with 30 kDa representing full-length KCTD6. Cullin-3 was found to be ubiquitously expressed throughout all analyzed tissue samples (middle). GAPDH was used as loading control (bottom). Asterisk indicates that the liver sample was diluted 1/10 for the KCTD6 blot. (B) Immunoblots of KCTD6 and sAnk1.5 expression in cardiac muscle at P0, P20, and adult stages indicates up-regulation of both proteins during postnatal development. (C) Analysis of sAnk1.5, KCTD6, cullin-3, sarcomeric myosin heavy chain (MyHC), and GAPDH protein levels during C2C12 differentiation. sAnk1.5 and KCTD6 display increased protein levels during C2C12 myotube development, as judged by expression of sarcomeric marker protein MyHC, while cullin-3 remains largely unchanged from undifferentiated myoblast stage (day 0). Note that the larger band in cullin-3 may represent nedd8-modified cullin-3. (D) Analysis of sAnk1.5, KCTD6, cullin-3, and obscurin protein localization in undifferentiated C2C12 myoblasts (day 0) and differentiated C2C12 myotubes. Note that despite overall down-regulation of cullin-3 levels in C2C12 cells (see C), cullin-3 expression levels appear higher in differentiated C2C12 cells (arrowhead in cullin-3 Day 0), when compared with neighboring undifferentiated cells (arrow in cullin-3 bottom). DAPI blue in overlay; sarcomeric marker α-actinin red in overlay. Scale bar: 20 μm.

sAnk1.5, KCTD6 and cullin-3 was also mirrored in immunofluorescence images of undifferentiated and differentiated C2C12 cells (Figure 5D). Analysis of the subcellular localization revealed that differentiating myoblasts display elevated cullin-3 in a vesicular pattern at day 0 and more diffusely at day 7 (Figure 5D, arrowhead in day 0, arrow in day 7 cullin-3 panel, respectively). The expression level of CSN5, a component of the COP9 signalosome that regulates cullin E3-ligase activity, remained comparable with undifferentiated myoblasts (Figure S4B).

In summary, KCTD6, sAnk1.5, cullin-3, and their associated proteins are expressed in muscle and developmentally up-regulated during sarcomerogenesis.

KCTD6 forms parallel homomeric complexes

Named for their tetramerization domain (BTB/POZ domain), which is homologous to homomeric interaction domains of potassium channels, KCTD proteins are thought to form tetramers. However, the crystal structure of KCTD5 yielded a surprising pentameric conformation (Dementieva *et al.*, 2009) despite being characterized earlier as a tetramer in biochemical experiments (Bayon *et al.*, 2008).

To understand KCTD6 binding, we investigated whether KCTD6 forms parallel or antiparallel complexes, and whether the KCTD6 C-terminus exhibits a conformational shape that could effectively block interaction with sAnk1.5 in nonmyogenic cells. Data from the protein complementation assay confirmed that KCTD6 forms parallel protein complexes in cells, bringing the N-termini of the individual KCTD6 proteins in close spatial vicinity (Figure S5A). We also found that KCTD6 is not assuming

a conformational "U" shape that would bring the KCTD6 N-terminus and C-terminus into proximity, thereby putatively blocking sAnk1.5 binding to the full-length KCTD6 BTB/POZ domain (Figure S5B). Using chemical cross-linking of full-length and C-terminally truncated KCTD6, we also analyzed whether KCTD6 forms tetrameric or pentameric complexes in cells. Full-length KCTD6 forms mainly dimeric and tetrameric complexes, as well as higher-order products (Figure S5C, left panel). No pentameric assemblies could be identified. C-terminally truncated KCTD6 is only able to form dimeric complexes in chemical cross-linking experiments (Figure S5C, right panel). As shown previously, the truncated dimeric form of KCTD6 BTB domain is able to interact with sAnk1.5 in nonmyogenic cells (Figure 1C). Taken together, these data indicate that the KCTD6 C-terminus may play important roles for complete tetramerization, and its ability to interact with other binding partners.

Analysis of KCTD6 interaction with its closest paralogue KCTD21 (Bayon *et al.*, 2008) and the well-characterized KCTD5 indicated absence of heteromer formation in either scenario (Figure S5D). These results agree with recent data on KCTD6 heteromerization (De Smaele *et al.*, 2011).

In summary, KCTD6 forms parallel homo-tetramers, with its N-terminal BTB/POZ domain being important for initial dimer formation, and its C-terminus being important for complete tetramerization/oligomerization and regulation of its interaction with cullin-3 substrate proteins.

KCTD6 regulates sAnk1.5 protein levels

Our results indicate that KCTD6 in combination with obscurin and cullin-3 may be important for small ankyrin protein turnover. Intriguingly, the degradation of RhoA, another protein that binds to the C-terminus of obscurin (Ford-Speelman *et al.*, 2009), is also dependent on cullin-3 and its interaction with another member of the KCTD protein family, KCTD13 (BACURD1; Chen *et al.*, 2009). Using RNA interference (RNAi), we investigated whether KCTD6 is necessary for sarcomerogenesis and protein turnover of the putative cullin-3 substrates sAnk1.5, as well as KCTD13- and obscurin-associated RhoA in neonatal rat cardiomyocytes (NRC).

Knockdown of KCTD6 in NRC resulted in significantly lowered KCTD6 protein levels of cells transfected with H1-rtKCTD6-green fluorescent protein (GFP; Figure 6A, top panels), whereas KCTD6 levels in untransfected or H1-GFP–transfected control cells remained unchanged (Figure 6A, bottom panel). RhoA displayed no changes in protein level or subcellular localization (Figure 6A, RhoA panels). Knockdown of KCTD6, however, dramatically increased sAnk1.5 protein levels (Figure 6B, top panel). Conversely, overexpression of KCTD6 was associated with a significant decrease of sAnk1.5 levels (Figure S6A). Sarcomerogenesis and myofibrillar maintenance were unaffected by KCTD6 knockdown, as judged by undisturbed α-actinin and obscurin staining (Figures 6B and S6B). Taken together, these data indicate that sAnk1.5 protein levels are inversely correlated to KCTD6 expression, and support the notion that sAnk1.5 protein turnover may be regulated by the UPS (Figure S6C) and cullin-3 substrate-linker functions of KCTD6.

Obscurin knockout animals exhibit changes in cullin and COP9 signalosome–associated proteins

We recently reported that skeletal muscles of obscurin knockout animals exhibit an abnormal SR architecture and develop a mild myopathy. A major hallmark in these mice was the altered localization and expression of sAnk1.5, which was found to be regulated on the protein, but not the mRNA, level (Lange *et al.*, 2009). Because knockdown of KCTD6 in cardiomyocytes was associated with up-regulation of sAnk1.5 protein levels, we wondered whether obscurin may exert an influence on cullin-3 and KCTD6. Several recent reports indicate that obscurin/UNC-89 and its close homologue Obsl1 are directly or indirectly linked to cullin E3 ligases (Benian, personal communication; Hanson *et al.*, 2009, 2011; Huber *et al.*, 2009; Litterman *et al.*, 2011).

To further examine the influence of obscurin on cullin, we investigated expression levels and localizations of sAnk1.5, KCTD6, cullin-3, and RhoA, in the obscurin knockout mice. All investigated proteins exhibited distinctive changes in localization in hearts of obscurin knockout animals (Figure 7A). Specifically, RhoA was entirely diffuse, and the M-band localization of KCTD6 was significantly diminished. Moreover, KCTD6 and cullin-3 displayed a marked increase in their association with the intercalated disk of obscurin knockout cardiomyocytes (Figure 7B). In contrast, expression levels of KCTD6 and cullin-3 remained mostly unaltered (Figure S7A). Notable, however, is the increase in p62/sequestosome-1 expression in heart and skeletal muscle of obscurin knockouts, indicating putative alterations to general protein turnover, ubiquitin signaling, and/or autophagy (Figure S7A, p62 panel).

DISCUSSION

The regulated turnover of proteins is fundamental for cell function. Deregulation of protein degradation is associated with developmental defects, impaired muscle differentiation, and embryonic lethality (Yue *et al.*, 2003; Witt *et al.*, 2008; Zhang *et al.*, 2009; Jang *et al.*, 2011). Proteins degraded by the UPS usually require polyubiquitylation by dedicated E3 ligases. For cullin-RING E3 ligases, substrate recognition and specificity are achieved through adaptor proteins, whereby each cullin has its own unique subset of linker protein families (Bosu and Kipreos, 2008): for example, cullin-3 depends on BTB/POZ domain–containing proteins for substrate recognition, whereas cullin-1 relies on Fbox domain–containing proteins, such as the muscle-specific FBXO32 (atrogin-1).

We identified KCTD6 as a novel binding partner of the muscle-specific ankyrin isoform sAnk1.5 (Figure 8A). Localization of sAnk1.5 and KCTD6 at the sarcomeric M-band in wild-type muscle, and the formation of a ternary KCTD6/sAnk1.5/obscurin complex in coimmunoprecipitation experiments (Figure S1C) further indicate that sAnk1.5 binding to KCTD6 may occur alongside its interaction with obscurin. The minimal binding side for KCTD6 could be located along the concave surface of the obscurin binding domain 2 (OBD-2) in sAnk1.5, facing away from the loop regions of the ankyrin-like repeats that form the interaction side with obscurin (Borzok *et al.*, 2007; Busby *et al.*, 2011). Another hypothesis for the simultaneous binding of KCTD6 and obscurin to sAnk1.5 is based on the oligomerization of sAnk1.5 (Figure S2F), whereby one molecule in the sAnk1.5 oligomer interacts with obscurin, while another could bind KCTD6. However, coimmunoprecipitation experiments using the Cys-22G/Cys-34G/Leu-44R/Gly/GlyR mutant sAnk1.5, which should prohibit sAnk1.5 oligomer formation, indicated that one sAnk1.5 molecule is able to bind KCTD6 and the obscurin-A C-terminus simultaneously (Figure S1C). Future experiments that study cocrystallization structures or molecular modeling may resolve this question more thoroughly.

We further demonstrated that sAnk1.5 can be posttranslationally modified by ubiquitin, nedd8, and acetylation that may be responsible for the muscle-specific interaction of sAnk1.5 with KCTD6. In contrast with a previous report indicating that neddylation of proteins may promote their ubiquitylation and subsequent degradation (Oved *et al.*, 2006), our protein complementation assays indicated that neddylation was not associated with increased turnover of sAnk1.5, as evidenced by detectable neddylation of sAnk1.5

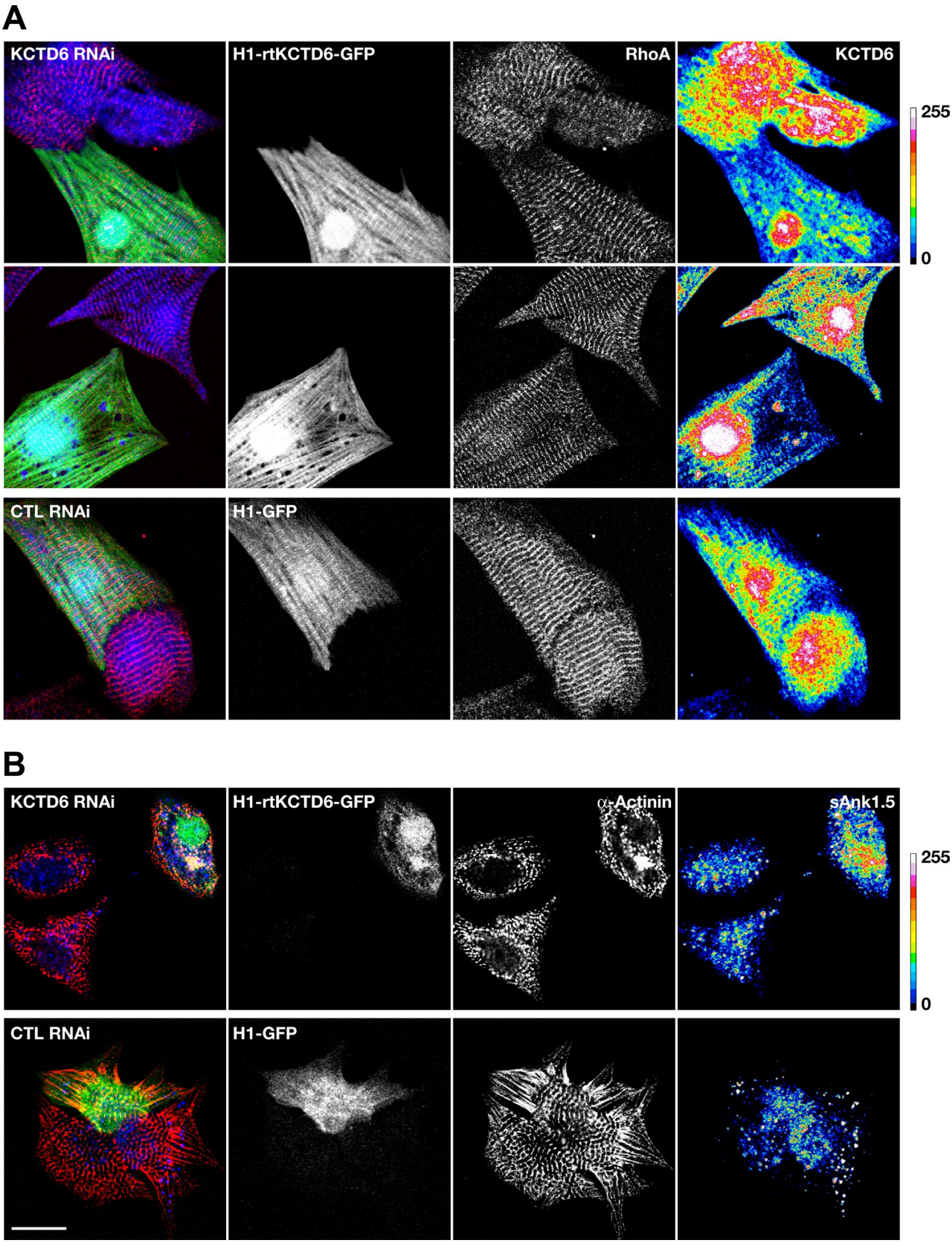

FIGURE 6: siRNA knockdown of KCTD6 in NRC. (A) siRNA-mediated knockdown of KCTD6 in NRC leads to reduced expression levels of endogenous KCTD6 when compared with either untransfected (KCTD6 RNAi; right panel, false-color overlay with signal intensity as displayed), or H1-GFP transfected control cells (bottom right panel). (B) Knockdown of endogenous KCTD6 results in increased expression level of endogenous sAnk1.5 (top panel, KCTD6 RNAi), when compared with untransfected (top right panels, false-color overlay with signal intensity as displayed) or H1-GFP–transfected control cells (bottom right panels). (A and B) Scale bar: 20 μm.

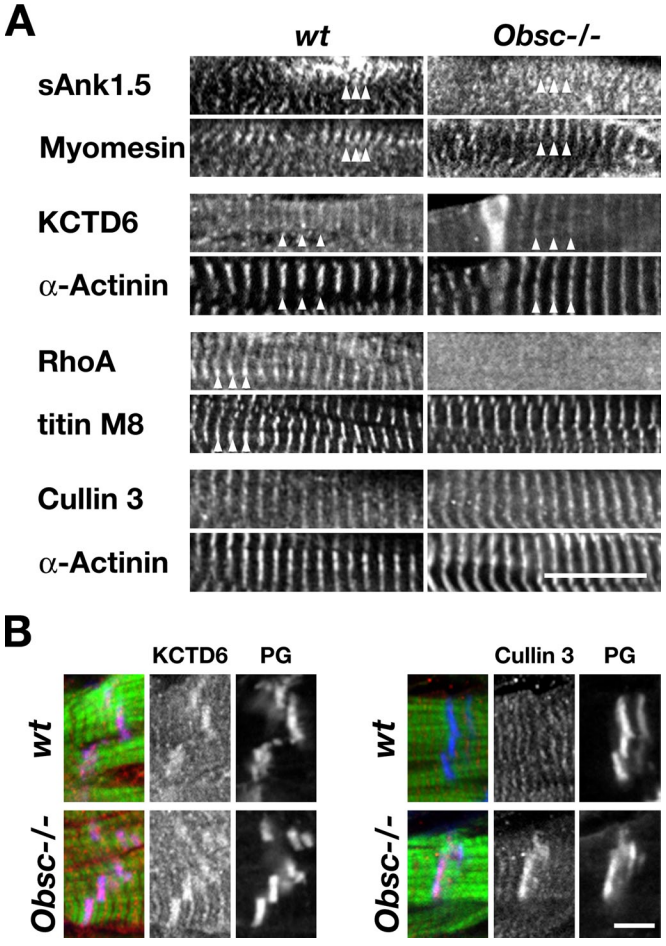

FIGURE 7: Analysis of sAnk1.5, KCTD6, cullin-3, and RhoA expression level and localization in obscurin knockout muscle. (A) Knockout of obscurin leads to changes in sAnk1.5, RhoA, KCTD6, and cullin-3 protein localization. Frozen sections of wild-type and obscurin knockout cross-striated muscle tissues were stained with antibodies directed against sAnk1.5, KCTD6, RhoA, and cullin-3. Prominent M-band localization of sAnk1.5, KCTD6, and RhoA in wild-type muscles appears abrogated in muscles from obscurin knockout animals. sAnk1.5 and RhoA are either diffuse or weakly associated to sarcomeric Z-disks in obscurin knockout muscles, whereas KCTD6 displays prominent Z-disk and intercalated disk association. Intriguingly, prominent localization of cullin-3 to sarcomeric Z-disks remains unchanged. Myomesin, titin-M8, and α-actinin were used as sarcomeric counterstains to show localization of sarcomeric M-band and Z-discs, respectively. Note that the sAnk1.5 staining for obscurin knockout muscles was recorded at higher gain settings compared with the wild-type muscle tissue to emphasize changes to sAnk1.5 localization. Indeed, sAnk1.5 levels were significantly decreased in obscurin knockout muscles (Lange *et al.*, 2009). Scale bar: 10 μm. (B) KCTD6 and cullin-3 localize to the intercalated disk in frozen sections of obscurin cardiac muscle. Cross-sections of muscle from wild-type and obscurin knockout hearts were stained with antibodies raised against KCTD6 and cullin-3 (red in overlay). Plakoglobin (γ-catenin) staining was used as intercalated disk (ID) marker (blue in overlay); F-actin was used to display sarcomeres (green in overlay). Scale bar: 6 μm.

without proteasome inhibitors. In contrast, polyubiquitylated sAnk1.5 was only visible after inhibition of the UPS by MG132. The observed differences between polyubiquitylation and neddylation of sAnk1.5 indicate that neddylation either serves an unrecognized function, or that nedd8 competitively occupies lysine residues needed for ubiquitylation.

Our binding assays and RNAi data and recent work done by others (De Smaele *et al.*, 2011) further indicate that KCTD6 may act as an sAnk1.5-specific substrate linker for cullin-3. The interaction of KCTD6 with cullin-3 and sAnk1.5 is dependent on its N-terminal BTB/POZ domain, which promotes dimerization of the protein. Further tetramerization/oligomerization of KCTD6 was dependent on the unstructured KCTD6 C-terminus that may also be responsible for the recognition of acetylated sAnk1.5, thereby exerting the observed tissue-specific binding of full-length KCTD6 to sAnk1.5.

Indeed, acetylation of proteins has been implicated as an avidity enhancer within interconnected multiprotein complexes (Scott *et al.*, 2011). Scott and colleagues describe how acetylation of an E2 ubiquitin-conjugating enzyme leads to neddylation, and thereby activation of cullin-1. Our findings, whereby acetylation of the substrate (sAnk1.5) promotes binding of the adaptor protein (KCTD6), thereby putatively enabling the assembly of the protein complex with the E3 ligase (cullin-3), fits this scheme. Although lysine acetylation of ankyrin 1 isoforms has been reported by tandem liquid chromatography–tandem mass spectrometry experiments (Zhao *et al.*, 2010), the biological function of acetylated ankyrin remains largely unknown. Surprisingly, increased acetylation of sAnk1.5 was not associated with increased sAnk1.5 turnover. While HDAC inhibition may exert side effects on components of the UPS on a global scale (Arendt and Hochstrasser, 1999), lysine acetylation has been shown to positively and negatively influence protein stability through different mechanisms (for a review, see Caron *et al.*, 2005). Future experiments may elucidate whether acetylation of substrates, linker proteins, and enzymes of the ubiquitin machinery acts as a general trigger for activation of protein degradation through cullin proteins.

One of the key findings in our analysis of the obscurin knockout was the decreased level and altered localization of sAnk1.5 in muscles of these mice (Lange *et al.*, 2009). While we observed decreased sAnk1.5 protein, but not mRNA, in obscurin knockouts, the mechanism by which this occurred remained unclear. Using the knowledge that KCTD6 and cullin-3 may be involved in sAnk1.5 turnover, we reexamined muscles from wild-type and obscurin knockouts. In wild-type, most of the KCTD6 staining colocalizes with sAnk1.5 and obscurin at the M-band, while cullin-3 resides exclusively at the Z-disk (Figure 8B, left). This spatial separation of sAnk1.5/KCTD6 and cullin-3 appears drastically altered in obscurin knockout muscles, in which sAnk1.5, KCTD6, and cullin-3 colocalize at the Z-disk/I-band region (Figure 8B, right), bringing the substrate (sAnk1.5) and its specific linker (KCTD6) in close spatial contact with the E3 ligase (cullin-3). Moreover, increased association of KCTD6 and cullin-3 at the intercalated disk in knockout hearts further suggests that absence of obscurin may have implications for other hitherto unidentified KCTD6 binding partners and potential cullin-3 substrates.

We also noted significant changes to p62/sequestosome-1 in obscurin knockouts. Because p62 is thought to link UPS-mediated protein degradation with autophagy (Bjorkoy *et al.*, 2009), alterations in p62 expression may indicate a general adaptation to protein turnover in obscurin knockout muscles. While the changed p62 expression levels and altered KCTD6 and cullin-3 localization may represent secondary changes in response to obscurin depletion, more direct links of obscurin family proteins with protein turnover have been observed. Direct association of the *C. elegans* obscurin homologue UNC-89 with cullin-1 (Benian, personal communication), and the interaction of the closely associated Obsl1 with cullin-7 (Litterman *et al.*, 2011) and its implication in the growth disorder 3-M syndrome (Hanson *et al.*, 2009; Huber *et al.*, 2009) may support the idea that obscurin/obsl1

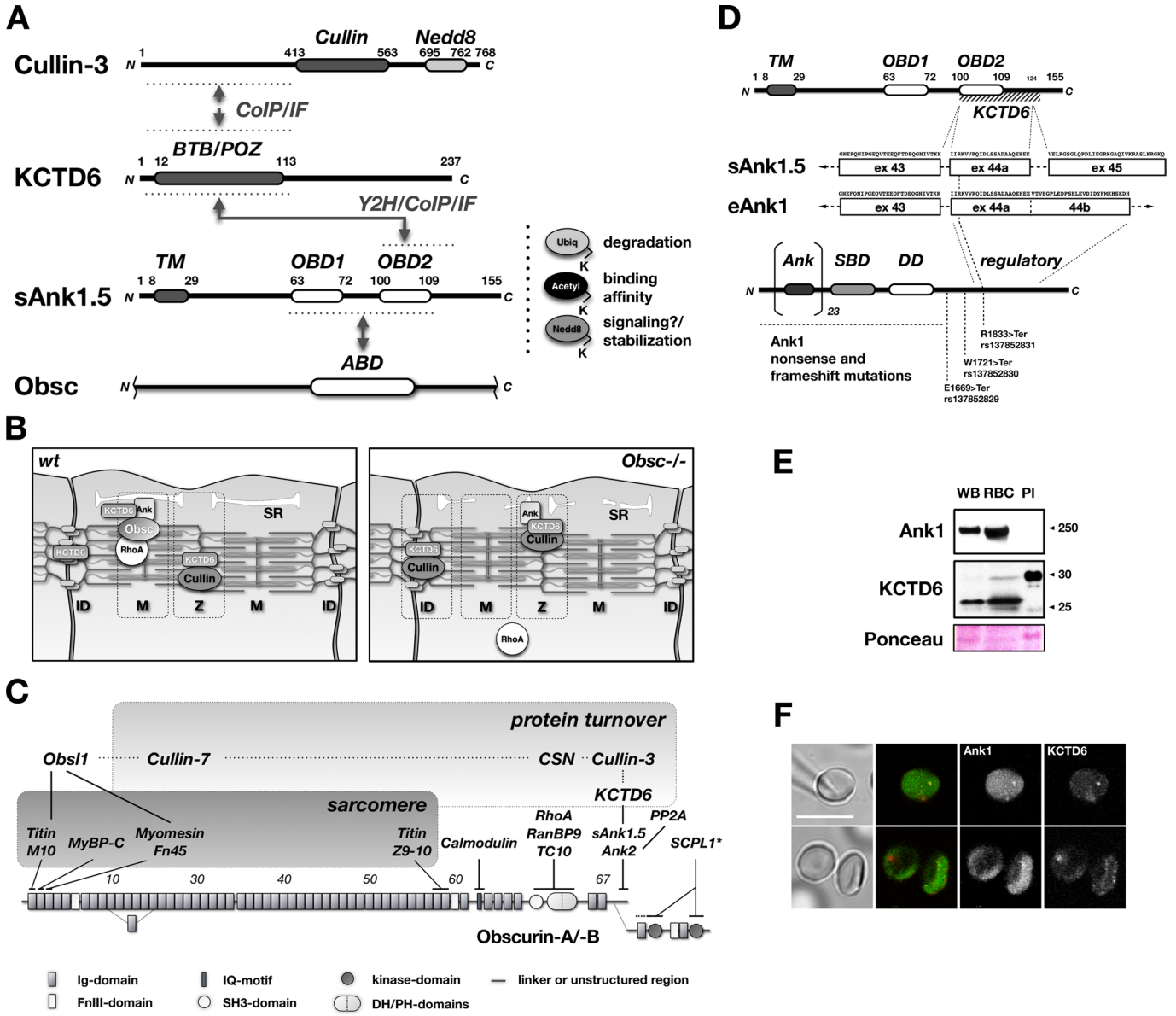

FIGURE 8: Summary of known and novel obscurin–sAnk1.5 protein interactions and posttranslational modifications. Changes to proteins in obscurin knockouts and a possible link to hereditary spherocytosis. (A) Summary of novel and known protein interactions. Domain structure of obscurin C-terminus, sAnk1.5, KCTD6, and cullin-3 and mapped minimal binding sites are indicated. Amino acid residues are for human sAnk1.5, KCTD6, and cullin-3. OBD, obscurin binding domain; ABD, ankyrin binding domain; TM, transmembrane domain; Obsc, obscurin. Posttranslational modification of sAnk1.5 by nedd8, ubiquitin, and acetylation of lysine residues is indicated. (B) Summary of sAnk1.5 (Ank), KCTD6, RhoA, and cullin protein localization changes between wild-type (left panel) and obscurin knockout heart muscles (right panel). ID, intercalated disk; M, M-band; Z, Z-disk; SR, sarcoplasmic reticulum. (C) Summary of obscurin domain layout and its protein interaction network, with novel and known protein interactions. Proteins involved in sarcomeric structure and protein turnover are grouped. (D) Mapping of KCTD6 site in sAnk1.5 reveals that the exon 44 encoding for the bulk of the binding region is also found in erythrocyte splice variants of Ank1 (eAnk1). Novel and known disease-associated Ank1 mutations that lead to C-terminal truncation of the protein may abrogate putative binding of KCTD6 to ankyrin-1 in erythrocytes. This finding raises the possibility of an involvement of KCTD6 in the development of Ank1-linked hereditary spherocytosis. Domain structure not to scale. Ank, ankyrin repeats; SBD, spectrin binding domain; DD, death domain. (E) Expression of Ank1 and KCTD6 in whole blood (WB), purified red blood cells (RBC), or blood plasma (Pl). The giant ankyrin-1 splice isoforms were detected in whole blood or purified red blood cells. A KCTD6 immunoreactive band at 30 kDa and approximately 25 kDa was detected in purified red blood cells. (F) KCTD6 partially colocalizes in red blood cells with ankyrin-1. Scale bar: 10 μm.

may directly and/or indirectly associate with and putatively regulate cullin-dependent protein turnover (Figure 8C). Moreover, Guy Benian and colleagues recently found a direct interaction of UNC-89 with MEL-26, a BTB/POZ-domain protein similar to KCTD6 that also interacts with cullin-3 (Wilson *et al.*, 2012). Whether obscurin and/or Obsl1 exert a regulatory function on

cullin-dependent protein turnover, a scaffolding function, or an as yet unidentified role for cullin remains to be characterized.

Another striking feature of obscurin knockout muscle is the diffuse localization of RhoA. While RhoA was recently characterized as a cullin-3 substrate through interaction with KCTD13 (Chen *et al.*, 2009), unaltered protein levels of RhoA in knockout muscles reason against an involvement of this pathway as a primary cause for the mislocalization of RhoA. Loss of RhoA binding to the SH3-DH-PH domains in obscurin (Ford-Speelman *et al.*, 2009) is the likely explanation for the drastically altered RhoA localization. Intriguingly, no physiological effects or myofibrillar defects (Lange *et al.*, 2009) were found associated with diffuse RhoA localization, rendering the association of RhoA with obscurin, its localization at the M-band, and its role in muscle biology more obscure.

During the identification of the minimal binding site of KCTD6 in human sAnk1.5, we noticed that exon 44a encompassing the region of ankyrin OBD-2 was also included in erythrocyte variants of human ANK1 (Figure 8D). Intriguingly, several known mutations affecting the giant erythrocyte ankyrin-1 isoforms may directly or indirectly impact the KCTD6 minimal binding site (del Giudice *et al.*, 1996; Eber *et al.*, 1996; Hughes *et al.*, 2011; Figure 8D, human single-nucleotide polymorphisms), mostly through premature termination and truncation of the ankyrin C-terminus. Particularly, the probably pathogenic polymorphism rs137852831 located at the extreme C-terminus of the regulatory domain of erythrocyte ANK1 leads to a truncation in the KCTD6 binding site (R1833X in human ANK1 isoform 3). Other nucleotide polymorphisms with unknown clinical relevance that are located within the mapped binding site of KCTD6 are rs143987736 and rs145506191, which result in the following mutations in ANK1 isoform 3: D1841N and A1843T, respectively. The expression of the KCTD6 binding site in erythrocyte ANK1 and the unknown disease mechanism of ankyrin-1 truncations in hereditary spherocytosis raise the possibility that KCTD6 may also interact with ankyrin-1 in erythrocytes and could be involved in the disease etiology. Indeed, KCTD6 is expressed in purified erythrocytes (Figure 8E), and colocalizes with ankyrin-1 along the red blood cell membrane (Figure 8F). Moreover, hereditary spherocytosis involving ANK1 gene mutations may be associated with altered levels of ankyrin binding partners spectrin and band-3 and associated proteins (Hughes *et al.*, 2011; Peker *et al.*, 2011). We speculate that pathological ANK1 mutations may be linked with the KCTD6/cullin-3 mediated ankyrin turnover mechanism described here. Ankyrin mutations may impair the ankyrin/KCTD6 interaction, resulting in altered stability of ankyrin-1 and its binding partners during erythrocyte development, leading to an impairment of the erythrocyte membrane cytoskeleton and ultimately, deformed red blood cells, as present in hereditary spherocytosis. It would be fascinating to investigate whether patients that suffer from hereditary spherocytosis and exhibit truncation of ankyrin-1 show concomitant changes in KCTD6 and cullin-3, as well as altered protein turnover in erythrocytes. Moreover, existence of patients that exhibit hereditary spherocytosis and symptoms of skeletal muscle myopathy (McCann and Jacob, 1976; Spencer *et al.*, 1987) and/or cardiomyopathy (Moiseyev *et al.*, 1987; Alter and Maisch, 2007; Finsterer and Stollberger, 2007) hint at a common molecular malfunction, potentially involving ankyrin-1 and KCTD6/cullin-3.

MATERIALS AND METHODS

Generation of constructs

KCTD6 and the cytoplasmic part of sAnk1.5 (residues 29–155) used for the yeast two-hybrid screen and the forced yeast two-hybrid assay were either cloned into pACT2 or pLexA vectors (Fukuzawa *et al.*, 2008) via PCR.

Generation of sAnk1.5, KCTD6, obscurin, Nedd8, ubiquitin, sumo1, and cullin-3 constructs for expression in eukaryotic cells, was done by PCR from a human cardiac cDNA library (Clontech, Mountain View, CA), and subcloning into the pEGFP-C1, pHA-N1, pHA-C1, and the protein complementation split–YFP vectors (Zou *et al.*, 2006) YN-C1, YC-N1, and YC-C1. The pHA-N1/C1 vectors were produced by in-frame replacement of the EGFP coding sequence in the pEGFP-N1/C1 vectors (Clontech) with the hemagglutinin (HA) tag (YPYDVPDYA). The construct for expression of sAnk1.5 in bacteria was done by in-frame integration of the cytoplasmic part of sAnk1.5 (residues 29–155) into pGST-C1, a modified pGEX-2TK vector, in which the multiple cloning site has been replaced with the multiple cloning site of the pEGFP-C1 vector. Generation of the construct for bacterial expression of His-tagged KCTD6 was done by subcloning human KCTD6 into the pTev vector (Pinotsis *et al.*, 2007), a modified version of the pET22b(+) vector (Novagen; Merck KGaA, Darmstadt, Germany), via PCR. The rat KCTD6 RNAi constructs were done by linker ligation of the following oligonucleotides (see Supplemental Table S1), into the H1-GFP vector (Fukuzawa *et al.*, 2008), a modified version of the pSUPER vector (kind gift of R. Agami, The Netherlands Cancer Institute, Amsterdam, The Netherlands; Brummelkamp *et al.*, 2002).

Site-directed mutagenesis of sAnk1.5 and KCTD6 constructs was done using a modified version of the QuickChange mutagenesis protocol (Stratagene, Agilent, Santa Clara, CA) and oligonucleotides harboring the desired mutation (Fukuzawa *et al.*, 2008).

All cDNAs and mutations were verified by sequencing. All residue numbers correspond to human sAnk1.5 (*Homo sapiens* ankyrin 1, transcript variant 5; National Center for Biotechnology Information [NCBI] accession number: NM_020478), human KCTD6 (NCBI accession number: NM_153331), and human cullin-3 (NCBI accession number: NM_003590).

Yeast two-hybrid assay

A yeast two-hybrid assay was done as previously described (Lange *et al.* 2002). pLexA-sAnk1.5 (29–155) was cotransformed with a pGAD10 human cardiac muscle cDNA library (Clontech) into the L40 yeast strain. Transformants were screened by *HIS3* and *LacZ* reporter gene activity. For forced yeast two-hybrid assays, pLexA-sAnk1.5 (residues 29–155, 29–137, 29–99, or 29–63) were cotransformed with either empty pACT2 vector or pACT2-KCTD6 (residues 1–147). After selection and growth of positive yeast transformants on minimal SD-medium lacking amino acids leucine and tryptophan, positive interaction was analyzed by *LacZ* reporter gene activity in an Xgal filter assay.

Cell culture

Cos-1 cells (Gluzman, 1981), C2C12 cells (Yaffe and Saxel, 1977), and NRCs were cultured as described previously (Lange *et al.*, 2002). NRC and Cos-1 cells at 80% confluency were transfected using ESCORT III (Sigma-Aldrich, St. Louis, MO) or Lipofectamine-2000 (Invitrogen, Life Technologies, Carlsbad, CA) following the manufacturers' manuals, and were harvested for immunofluorescence, coimmunoprecipitation, and/or immunoblot analysis 48 h after transfection. C2C12 cells in the myoblast stage were transfected using Lipofectamine-2000. C2C12 cells were changed from growth medium (20% FCS, DMEM, 1× penicillin/streptomycin) into differentiation medium (2% horse serum, DMEM, 1× penicillin/streptomycin) 24 h after transfection, and then differentiated for 1–12 d.

KCTD6 RNAi was done by transfection of a rat-specific KCTD6 H1-GFP vector by using ESCORT III into NRC. The effect of small interfering RNA (siRNA) was assessed 5 d after transfection.

Treatment of cells with HDAC inhibitor was done by supplementing the growth medium with 0.5 μg/ml TSA (Sigma-Aldrich) for 4–24 h. Investigation of protein degradation was done by supplementing cell culture medium with either 10 μM MG132 (Santa Cruz Biotechnology, Santa, Cruz, CA) and culturing cells for 3–24 h, or with 10 μg/ml cycloheximide (CHX; Santa Cruz Biotechnology) and culturing cells for 6 h. For analysis of protein phosphorylation, cells were incubated with 200 nM staurosporine (Sigma-Aldrich) in cell culture medium for 1 h.

Immunostaining and microscopy

Immunostaining of frozen sections and cells was done as previously described (Lange *et al.*, 2002). Immunostaining of frozen cardiac sections was done by fixing cross-sections (10 μm) in ice-cold acetone for 5 min at −20°C, which was followed by rehydration in 1X phosphate-buffered saline (PBS) for 5 min at room temperature. After permeabilization (0.2% Triton X-100 for 5 min at room temperature), sections were incubated with a mixture of primary antibodies in gold buffer (GB; 20 mM Tris-HCl, pH 7.5, 155 mM NaCl, 2 mM ethylene glycol tetraacetic acid, 2 mM $MgCl_2$, 5% bovine serum albumin [BSA]) overnight at 4°C. After being washed with PBS, the sections were transferred into the secondary antibody mixture (in GB), incubated for 1 h at room temperature, washed again with PBS, and finally mounted in fluorescent mounting medium (Dako, Carpinteria, CA). Immunostaining of Cos-1, C2C12, NRC, and diaphragm whole mounts was done using a similar protocol, but the acetone fixation step was replaced with a 4% PFA/PBS fixation for 5–15 min at room temperature. Immunostaining of red blood cells was performed after isolation and purification of intact erythrocytes from whole blood by centrifugation at 1000 × *g* in a tabletop centrifuge for 1 min, transfer of the red blood cell fraction to a new tube, and washing of erythrocytes with PBS. Fixation of erythrocytes was done by resuspending and incubating red blood cells in 2% glutaraldehyde, 2% PFA in 0.15M cacodylate buffer (pH 7.4) for 10 min at room temperature. After fixation, red blood cells were permeabilized for 5 min with 0.1% triton in PBS and stained in suspension with primary antibodies diluted in PBS supplemented with 1% BSA for 2 h at room temperature, which was followed by three washes using PBS and labeling with secondary antibodies diluted in PBS with 1% BSA. Cells were washed three times with PBS and mounted on coverslips in PBS for confocal microscopy. Samples were imaged using an Olympus Fluoview confocal microscope in sequential scanning mode using 40× or 60× oil-immersion objectives and zoom rates between 1 and 4.

Sequence analysis, image analysis, and statistical analysis

Secondary-structure analysis was done using the Web-based prediction software JPRED3 (University of Dundee, United Kingdom; www.compbio.dundee.ac.uk/~www-jpred). Prediction of putative phosphorylation sites was done using NetPhos (Blom *et al.*, 1999; www.cbs.dtu.dk/services/NetPhos) or phosphosite (Cell Signaling Technology, Danvers, MA; www.phosphosite.org). Domain prediction was done using SMART (Schultz *et al.*, 1998; European Molecular Biology Laboratory; http://smart.embl-heidelberg.de). Helical wheel projections were done using a Web-based software created by Don Armstrong (http://rzlab.ucr.edu/scripts/wheel/wheel.cgi).

Densitometric analysis of immunoblots and ratiometric analysis of fluorescent images was done using ImageJ (National Institutes of Health [NIH]). For visualization of protein levels in NRCs transfected with RNAi constructs, look-up tables in channels depicting KCTD6 or sAnk1.5 were changed in ImageJ to 16 colors (16_colors.lut; shown in the intensity scale in Figure 6 and Supplemental Figure S6A). Statistical analysis was done using Excel (Microsoft, Redmond, WA). Significance was determined using analysis of variance calculation with a significance level of 0.05 or 0.01. Results are presented as means ± SE. Number of measurements (n) and p values are shown in the figures or legends.

Antibodies

Antibodies raised against human KCTD6 were obtained from Abcam (Cambridge, MA; ab62596). Polyclonal mouse anti-KCTD6 antibodies were generated in-house by intramuscular injection of a 1:1 mixture of 2 mg His-tagged human KCTD6-BTB domain and TiterMax Gold adjuvant (Sigma-Aldrich) into mice. Three months following the injection, mouse serum was collected and tested for immunoreactivity. Antibodies raised against sAnk1.5 were obtained from Aviva Sysbio (ARP42566_T100). Antibodies raised against GFP and HA tags were obtained from Roche (Indianapolis, IN). The antibody recognizing an obscurin epitope in domains IQ-Ig64 was generated in our laboratory (Lange *et al.*, 2009). Additionally, the following mouse, goat, and rabbit antibodies were used in this study: myomesin-B4 (Developmental Studies Hybridoma Bank [DSHB] University of Iowa, developed by J. C. Perriard, ETH Zurich, Zurich, Switzerland), α-actinin (clone EA53; Sigma-Aldrich), titin-M8 (developed by Mathias Gautel, King's College London, United Kingdom), nedd8 (Sigma-Aldrich), cullin-3 (Sigma-Aldrich), Skp1 (Santa Cruz Biotechnology), CSN5 (Santa Cruz Biotechnology), MyHC (clone 1025; DSHB University of Iowa, developed by H. Blau, Stanford University, Stanford, CA), RhoA (Santa Cruz Biotechnology), p62 (BD-Transduction, San Jose, CA), GAPDH (Santa Cruz Biotechnology), β-tubulin (clone E7; DSHB University of Iowa, developed by M. Klymkowsky, University of Colorado, Boulder, CO), plakoglobin (BD-Transduction), and acetyl-lysine (Cell Signaling Technology). All fluorescently or enzymatically (horseradish peroxidase) labeled secondary antibodies were from either Dako or Jackson ImmunoResearch (West Grove, PA).

For immunofluorescence, 4′,6-diamidino-2-phenylindole (DAPI; 2 mg/ml; Sigma-Aldrich) or fluorescently labeled phalloidin (Molecular Probes) was incubated with the secondary antibody mixture.

Coimmunoprecipitation and GST-pulldown assays

Biochemical protein–protein interaction assays were performed as described previously (Lange *et al.*, 2002). Bacterial expression was done in BL21 Star cells (Invitrogen) following standard procedures (Lange *et al.*, 2002). For GST-pulldown assays, purified GST-tagged sAnk1.5 (residues 29–155) in IP buffer (150 mM NaCl, Tris-HCl pH 8, 1 mM DTT, 1× Complete Protease Inhibitor EDTA-free [Roche], 0.2% NP-40) was bound to glutathione Sepharose 4B resin (Pharmacia). For coimmunoprecipitations, soluble immunocomplexes in IP buffer were bound to protein G–linked magnetic beads (Dynabeads; Invitrogen). Following binding of the protein–protein complexes or protein–immunocomplexes and incubation at 4°C for 2 h with agitation, beads were washed three times with IP buffer, resuspended in SDS sample buffer, and analyzed by SDS–PAGE, which was followed by immunoblotting onto nitrocellulose membranes (Schleicher & Schuell or Bio-Rad, Hercules, CA).

Protein analysis and cross-linking

To generate protein samples from transfected or untransfected Cos-1, C2C12, or NRC, cells were washed once in PBS and directly lysed in SDS-sample buffer. Mouse tissue samples were homogenized directly in SDS sample buffer (1:40 tissue weight [mg]:SDS-sample buffer volume [ml] ratio) using a polytron-blade homogenizer (Pro Scientific). Protein levels were equalized by adjusting protein amounts according to actin, β-tubulin, or GAPDH intensity.

For mobility shift assays, HA-tagged sAnk1.5 or KCTD6 was transfected with or without GFP-tagged nedd8 or sumo-1. At 48 h after transfection, proteins were harvested directly in SDS-sample buffer and analyzed on SDS–PAGE; this was followed by immunoblot analysis.

For treatment of proteins with shrimp alkaline phosphatase (SAP), transfected cells were washed once in PBS and lysed in IP buffer. After separation of the soluble and insoluble fraction by centrifugation at 14,000 rpm in a tabletop centrifuge at 4°C, soluble proteins were incubated with 26 U/ml of SAP (Roche) for 45 min at 37°C. After proteins were mixed with SDS-sample buffer, they were separated on SDS–PAGE; this was followed by immunoblot analysis.

Chemical cross-linking of protein lysates from transfected Cos-1 cells was done as described previously (Lange *et al.*, 2005a). Lysates from transfected Cos-1 cells containing soluble fractions of HA-tagged full-length KCTD6 or KCTD6 N-terminal BTB domain were changed from IP buffer (see *Coimmunoprecipitation and GST-pulldown assays* section) into PBS using Zeba Spin columns (Pierce, Rockford, IL). After addition of chemical cross-linker ethylene glycol bis(succinimido succinate); Sigma-Aldrich) to a final concentration of 1.3 mM and incubation of protein samples at 37°C for 15 min, proteins were precipitated by adding 12% trichloroacetic acid (1:1 ratio). Proteins were pelleted for 10 min at 4°C using a tabletop microcentrifuge, and the protein pellet was redissolved in SDS sample buffer and separated by SDS–PAGE; this was followed by immunoblot analysis.

Mice

Generation of obscurin knockout mice has been described previously (Lange *et al.*, 2009). All procedures involving mice were done in accordance with the Institutional Animal Care and Use Committee, NIH, and Association for Assessment and Accreditation of Laboratory Animal Care regulations under the observance and care of trained animal staff and veterinarians.

ACKNOWLEDGMENTS

S.L. was funded by a development grant of the Muscular Dystrophy Association (MDA68929) and an NIH K99/R00 Pathway to Independence Award (1K99HL107744-01). Parts of this work were supported by a University of California, San Diego (UCSD), Cardiovascular Fellowship awarded to S.L. J.C. is funded by grants from the National Institute of Arthritis and Musculoskeletal and Skin Diseases (R01AR059334) and the National Heart, Lung, and Blood Institute. J.C. is the American Heart Association Endowed Chair in Cardiovascular Research. Sue Perera is funded by the Medical Research Council and BHF. Funding for the UCSD Microscopy and Stem Cell Facility was provided by grants from the NIH (P30-NS047101 and P30-CA23100). We thank Enrico Girardi (La Jolla Institute for Allergy and Immunology), Elisabeth Ehler (King's College London), Mathias Gautel (King's College London), and Guy Benian (Emory University) for critical discussions. We acknowledge the DSHB (University of Iowa) for provision of the myomesin-B4 and β-tubulin antibodies.

REFERENCES

Alter P, Maisch B (2007). Non-compaction cardiomyopathy in an adult with hereditary spherocytosis. Eur J Heart Fail 9, 98–99.

Arendt CS, Hochstrasser M (1999). Eukaryotic 20S proteasome catalytic subunit propeptides prevent active site inactivation by N-terminal acetylation and promote particle assembly. EMBO J 18, 3575–3585.

Bagnato P, Barone V, Giacomello E, Rossi D, Sorrentino V (2003). Binding of an ankyrin-1 isoform to obscurin suggests a molecular link between the sarcoplasmic reticulum and myofibrils in striated muscles. J Cell Biol 160, 245–253.

Bang ML *et al.* (2001). The complete gene sequence of titin, expression of an unusual approximately 700-kDa titin isoform, and its interaction with obscurin identify a novel Z-line to I-band linking system. Circ Res 89, 1065–1072.

Bayon Y *et al.* (2008). KCTD5, a putative substrate adaptor for cullin3 ubiquitin ligases. FEBS J 275, 3900–3910.

Bjorkoy G, Lamark T, Pankiv S, Overvatn A, Brech A, Johansen T (2009). Monitoring autophagic degradation of p62/SQSTM1. Methods Enzymol 452, 181–197.

Blom N, Gammeltoft S, Brunak S (1999). Sequence and structure-based prediction of eukaryotic protein phosphorylation sites. J Mol Biol 294, 1351–1362.

Borzok MA, Catino DH, Nicholson JD, Kontrogianni-Konstantopoulos A, Bloch RJ (2007). Mapping the binding site on small ankyrin 1 for obscurin. J Biol Chem 282, 32384–32396.

Bosu DR, Kipreos ET (2008). Cullin-RING ubiquitin ligases: global regulation and activation cycles. Cell Div 3, 7.

Bowman AL, Catino DH, Strong JC, Randall WR, Kontrogianni-Konstantopoulos A, Bloch RJ (2008). The rho-guanine nucleotide exchange factor domain of obscurin regulates assembly of titin at the Z-disk through interactions with Ran binding protein 9. Mol Biol Cell 19, 3782–3792.

Brummelkamp TR, Bernards R, Agami R (2002). A system for stable expression of short interfering RNAs in mammalian cells. Science 296, 550–553.

Busby B, Oashi T, Willis CD, Ackermann MA, Kontrogianni-Konstantopoulos A, Mackerell AD, Jr., Bloch RJ (2011). Electrostatic interactions mediate binding of obscurin to small ankyrin 1: biochemical and molecular modeling studies. J Mol Biol 408, 321–334.

Caron C, Boyault C, Khochbin S (2005). Regulatory cross-talk between lysine acetylation and ubiquitination: role in the control of protein stability. Bioessays 27, 408–415.

Centner T *et al.* (2001). Identification of muscle specific ring finger proteins as potential regulators of the titin kinase domain. J Mol Biol 306, 717–726.

Chang TL, Cubillos FF, Kakhniashvili DG, Goodman SR (2004). Ankyrin is a target of spectrin's E2/E3 ubiquitin-conjugating/ligating activity. Cell Mol Biol (Noisy-le-grand) 50, 59–66.

Chen Y, Yang Z, Meng M, Zhao Y, Dong N, Yan H, Liu L, Ding M, Peng HB, Shao F (2009). Cullin mediates degradation of RhoA through evolutionarily conserved BTB adaptors to control actin cytoskeleton structure and cell movement. Mol Cell 35, 841–855.

del Giudice EM, Hayette S, Bozon M, Perrotta S, Alloisio N, Vallier A, Iolascon A, Delaunay J, Morle L (1996). Ankyrin Napoli: a de novo deletional frameshift mutation in exon 16 of ankyrin gene (ANK1) associated with spherocytosis. Br J Haematol 93, 828–834.

Dementieva IS, Tereshko V, McCrossan ZA, Solomaha E, Araki D, Xu C, Grigorieff N, Goldstein SA (2009). Pentameric assembly of potassium channel tetramerization domain-containing protein 5. J Mol Biol 387, 175–191.

De Smaele E *et al.* (2011). Identification and characterization of KCASH2 and KCASH3, 2 novel Cullin3 adaptors suppressing histone deacetylase and Hedgehog activity in medulloblastoma. Neoplasia 13, 374–385.

Eber SW *et al.* (1996). Ankyrin-1 mutations are a major cause of dominant and recessive hereditary spherocytosis. Nat Genet 13, 214–218.

Finsterer J, Stollberger C (2007). Myopathy associated with spherocytosis and left ventricular hypertrabeculation/noncompaction. Eur J Heart Fail 9, 100 [author reply, 101].

Ford-Speelman DL, Roche JA, Bowman AL, Bloch RJ (2009). The rho-guanine nucleotide exchange factor domain of obscurin activates rhoA signaling in skeletal muscle. Mol Biol Cell 20, 3905–3917.

Fukuzawa A, Lange S, Holt M, Vihola A, Carmignac V, Ferreiro A, Udd B, Gautel M (2008). Interactions with titin and myomesin target obscurin and obscurin-like 1 to the M-band: implications for hereditary myopathies. J Cell Sci 121, 1841–1851.

Gallagher PG, Forget BG (1998). An alternate promoter directs expression of a truncated, muscle-specific isoform of the human ankyrin 1 gene. J Biol Chem 273, 1339–1348.

Geisler SB, Robinson D, Hauringa M, Raeker MO, Borisov AB, Westfall MV, Russell MW (2007). Obscurin-like 1, OBSL1, is a novel cytoskeletal protein related to obscurin. Genomics 89, 521–531.

Gluzman Y (1981). SV40-transformed simian cells support the replication of early SV40 mutants. Cell 23, 175–182.

Gomes MD, Lecker SH, Jagoe RT, Navon A, Goldberg AL (2001). Atrogin-1, a muscle-specific F-box protein highly expressed during muscle atrophy. Proc Natl Acad Sci USA 98, 14440–14445.

Hanson D *et al.* (2011). Exome sequencing identifies CCDC8 mutations in 3-M syndrome, suggesting that CCDC8 contributes in a pathway with CUL7 and OBSL1 to control human growth. Am J Hum Genet 89, 148–153.

Hanson D *et al.* (2009). The primordial growth disorder 3-M syndrome connects ubiquitination to the cytoskeletal adaptor OBSL1. Am J Hum Genet 84, 801–806.
Hassink RJ, Nakajima H, Nakajima HO, Doevendans PA, Field LJ (2009). Expression of a transgene encoding mutant p193/CUL7 preserves cardiac function and limits infarct expansion after myocardial infarction. Heart 95, 1159–1164.
Hsieh CM, Fukumoto S, Layne MD, Maemura K, Charles H, Patel A, Perrella MA, Lee ME (2000). Striated muscle preferentially expressed genes α and β are two serine/threonine protein kinases derived from the same gene as the aortic preferentially expressed gene-1. J Biol Chem 275, 36966–36973.
Hsu YJ, Goodman SR (2005). Spectrin and ubiquitination: a review. Cell Mol Biol (Noisy-le-grand) Suppl 51, OL801–OL807.
Huber C *et al.* (2009). OBSL1 mutations in 3-M syndrome are associated with a modulation of IGFBP2 and IGFBP5 expression levels. Hum Mutat 31, 20–26.
Hughes MR *et al.* (2011). A novel ENU-generated truncation mutation lacking the spectrin-binding and C-terminal regulatory domains of Ank1 models severe hemolytic hereditary spherocytosis. Exp Hematol 39, 305–320 [correction published in Exp Hematol (2011). 39, 601].
Jang JW, Lee WY, Lee JH, Moon SH, Kim CH, Chung HM (2011). A novel Fbxo25 acts as an E3 ligase for destructing cardiac specific transcription factors. Biochem Biophys Res Commun 410, 183–188.
Kamitani T, Kito K, Nguyen HP, Yeh ET (1997). Characterization of NEDD8, a developmentally down-regulated ubiquitin-like protein. J Biol Chem 272, 28557–28562.
Kontrogianni-Konstantopoulos A, Jones EM, Van Rossum DB, Bloch RJ (2003). Obscurin is a ligand for small ankyrin 1 in skeletal muscle. Mol Biol Cell 14, 1138–1148.
Lange S, Auerbach D, McLoughlin P, Perriard E, Schafer BW, Perriard JC, Ehler E (2002). Subcellular targeting of metabolic enzymes to titin in heart muscle may be mediated by DRAL/FHL-2. J Cell Sci 115, 4925–4936.
Lange S, Himmel M, Auerbach D, Agarkova I, Hayess K, Furst DO, Perriard JC, Ehler E (2005a). Dimerisation of myomesin: implications for the structure of the sarcomeric M-band. J Mol Biol 345, 289–298.
Lange S, Ouyang K, Meyer G, Cui L, Cheng H, Lieber RL, Chen J (2009). Obscurin determines the architecture of the longitudinal sarcoplasmic reticulum. J Cell Sci 122, 2640–2650.
Lange S *et al.* (2005b). The kinase domain of titin controls muscle gene expression and protein turnover. Science 308, 1599–1603.
Li HH, Kedar V, Zhang C, McDonough H, Arya R, Wang DZ, Patterson C (2004). Atrogin-1/muscle atrophy F-box inhibits calcineurin-dependent cardiac hypertrophy by participating in an SCF ubiquitin ligase complex. J Clin Invest 114, 1058–1071.
Litterman N, Ikeuchi Y, Gallardo G, O'Connell BC, Sowa ME, Gygi SP, Harper JW, Bonni A (2011). An OBSL1-Cul7Fbxw8 ubiquitin ligase signaling mechanism regulates Golgi morphology and dendrite patterning. PLoS Biol 9, e1001060.
Liu X *et al.* (2009). Disruption of striated preferentially expressed gene locus leads to dilated cardiomyopathy in mice. Circulation 119, 261–268.
Martinez-Vicente M, Sovak G, Cuervo AM (2005). Protein degradation and aging. Exp Gerontol 40, 622–633.
McCann SR, Jacob HS (1976). Spinal cord disease in hereditary spherocytosis: report of two cases with a hypothesized common mechanism for neurologic and red cell abnormalities. Blood 48, 259–263.
McElhinny AS, Kakinuma K, Sorimachi H, Labeit S, Gregorio CC (2002). Muscle-specific RING finger-1 interacts with titin to regulate sarcomeric M-line and thick filament structure and may have nuclear functions via its interaction with glucocorticoid modulatory element binding protein-1. J Cell Biol 157, 125–136.
Miller RK, Qadota H, Landsverk ML, Mercer KB, Epstein HF, Benian GM (2006). UNC-98 links an integrin-associated complex to thick filaments in *Caenorhabditis elegans* muscle. J Cell Biol 175, 853–859.
Miller RK, Qadota H, Stark TJ, Mercer KB, Wortham TS, Anyanful A, Benian GM (2009). CSN-5, a component of the COP9 signalosome complex, regulates the levels of UNC-96 and UNC-98, two components of M-lines in *Caenorhabditis elegans* muscle. Mol Biol Cell 20, 3608–3616.
Moiseyev VS, Korovina EA, Polotskaya EL, Poliyanskaya IS, Yazdovsky VV (1987). Hypertrophic cardiomyopathy associated with hereditary spherocytosis in three generations of one family. Lancet 2, 853–854.
Mrosek M, Labeit D, Witt S, Heerklotz H, von Castelmur E, Labeit S, Mayans O (2007). Molecular determinants for the recruitment of the ubiquitin-ligase MuRF-1 onto M-line titin. FASEB J 21, 1383–1392.
Muller S, Lange S, Gautel M, Wilmanns M (2007). Rigid conformation of an immunoglobulin domain tandem repeat in the A-band of the elastic muscle protein titin. J Mol Biol 371, 469–480.
Nakajima H, Nakajima HO, Tsai SC, Field LJ (2004). Expression of mutant p193 and p53 permits cardiomyocyte cell cycle reentry after myocardial infarction in transgenic mice. Circ Res 94, 1606–1614.
Oved S *et al.* (2006). Conjugation to Nedd8 instigates ubiquitylation and down-regulation of activated receptor tyrosine kinases. J Biol Chem 281, 21640–21651.
Pan ZQ, Kentsis A, Dias DC, Yamoah K, Wu K (2004). Nedd8 on cullin: building an expressway to protein destruction. Oncogene 23, 1985–1997.
Peker S, Akar N, Demiralp DO (2011). Proteomic identification of erythrocyte membrane protein deficiency in hereditary spherocytosis. Mol Biol Rep 39, 3161–3167.
Perera S, Holt MR, Mankoo BS, Gautel M (2011). Developmental regulation of MURF ubiquitin ligases and autophagy proteins nbr1, p62/SQSTM1 and LC3 during cardiac myofibril assembly and turnover. Dev Biol 351, 46–61.
Pinotsis N, Lange S, Perriard JC, Svergun DI, Wilmanns M (2007). Molecular basis of the C-terminal tail-to-tail assembly of the sarcomeric filament protein myomesin. EMBO J 27, 253–264.
Porter NC, Resneck WG, O'Neill A, Van Rossum DB, Stone MR, Bloch RJ (2005). Association of small ankyrin 1 with the sarcoplasmic reticulum. Mol Membr Biol 22, 421–432.
Schultz J, Milpetz F, Bork P, Ponting CP (1998). SMART, a simple modular architecture research tool: identification of signaling domains. Proc Natl Acad Sci USA 95, 5857–5864.
Scott DC, Monda JK, Bennett EJ, Harper JW, Schulman BA (2011). N-terminal acetylation acts as an avidity enhancer within an interconnected multiprotein complex. Science 334, 674–678.
Spencer JA, Eliazer S, Ilaria RL, Jr., Richardson JA, Olson EN (2000). Regulation of microtubule dynamics and myogenic differentiation by MURF, a striated muscle RING-finger protein. J Cell Biol 150, 771–784.
Spencer SE, Walker FO, Moore SA (1987). Chorea-amyotrophy with chronic hemolytic anemia: a variant of chorea-amyotrophy with acanthocytosis. Neurology 37, 645–649.
Su H, Li J, Menon S, Liu J, Kumarapeli AR, Wei N, Wang X (2010). Perturbation of cullin deneddylation via conditional Csn8 ablation impairs the ubiquitin-proteasome system and causes cardiomyocyte necrosis and dilated cardiomyopathy in mice. Circ Res 108, 40–50.
Su H, Wang X (2010). The ubiquitin-proteasome system in cardiac proteinopathy: a quality control perspective. Cardiovasc Res 85, 253–262.
Wilson KJ, Qadota H, Mains PE, Benian GM (2012). UNC-89 (obscurin) binds to MEL-26, a BTB-domain protein, and affects the function of MEI-1 (katanin) in striated muscle of *Caenorhabditis elegans*. Mol Biol Cell (*in press*).
Witt CC, Witt SH, Lerche S, Labeit D, Back W, Labeit S (2008). Cooperative control of striated muscle mass and metabolism by MuRF1 and MuRF2. EMBO J 27, 350–360.
Witt SH, Granzier H, Witt CC, Labeit S (2005). MURF-1 and MURF-2 target a specific subset of myofibrillar proteins redundantly: towards understanding MURF-dependent muscle ubiquitination. J Mol Biol 350, 713–722.
Yaffe D, Saxel O (1977). Serial passaging and differentiation of myogenic cells isolated from dystrophic mouse muscle. Nature 270, 725–727.
Young P, Ehler E, Gautel M (2001). Obscurin, a giant sarcomeric Rho guanine nucleotide exchange factor protein involved in sarcomere assembly. J Cell Biol 154, 123–136.
Yue Z, Jin S, Yang C, Levine AJ, Heintz N (2003). Beclin 1, an autophagy gene essential for early embryonic development, is a haploinsufficient tumor suppressor. Proc Natl Acad Sci USA 100, 15077–15082.
Zhang Q, Wang K, Zhang Y, Meng J, Yu F, Chen Y, Zhu D (2009). The myostatin-induced E3 ubiquitin ligase RNF13 negatively regulates the proliferation of chicken myoblasts. FEBS J 277, 466–476.
Zhao S *et al.* (2010). Regulation of cellular metabolism by protein lysine acetylation. Science 327, 1000–1004.
Zou P, Pinotsis N, Lange S, Song YH, Popov A, Mavridis I, Mayans OM, Gautel M, Wilmanns M (2006). Palindromic assembly of the giant muscle protein titin in the sarcomeric Z-disk. Nature 439, 229–233.